A MATHEMATICAL MODEL OF STEADY FLOW IN CURVED SHALLOW CHANNELS

H.J. de Vriend

Report no. 76-1

Laboratory of Fluid Mechanics

Delft University of Technology

Department of Civil Engineering

Delft, the Netherlands.

CONTENTS

Figures

SAMENVATTING

Uitgaande van de Reynoldsvergelijkingen met de bijbehorende randvoorwaarden wordt een vereenvoudigd wiskundig model afgeleid voor ondiepe bochtige rivieren, met als voornaamste uitgangspunten:

- de vertikale afgeleiden van de snelheden zijn groot t.o.v. de horizontale
- de schuifspanningseffekten overheersen de traagheids- (advectieve) effekten.

Dit lijkt juist voor het geval dat de waterdiepte klein is t.o.v. de breedte en de representatieve bochtstraal, terwijl niet te sterke variaties in de geometrie mogen optreden.
Het aldus verkregen stelsel differentiaalvergelijkingen met randvoorwaarden is in twee stappen oplosbaar. Eerst wordt (analytisch) de vertikale verdeling van de snelheidscomponenten en de totale druk bepaald, d.w.z. de vorm van de krommen maar nog niet de numerieke waarden. Met gebruikmaking van deze informatie worden vervolgens de vergelijkingen geïntegreerd over de waterdiepte, waarna de over de diepte gemiddelde waarden van snelheden en druk berekend worden door het geïntegreerde stelsel numeriek op te lossen.
Bij vergelijking van de resultaten met metingen blijkt het gebruikte model goed te voldoen voor wat betreft de verdelingen in de vertikaal, maar minder goed waar het gaat om de verdeling van de gemiddelde grootheden, vooral bij vlakke bodem. Dit is kwalitatief te verklaren uit het feit dat het advectieve effekt van de secundaire stroming op de hoofdstroom en de invloed van de oevers niet in het model zijn opgenomen.

I. INTRODUCTION

The steady flow in a river usually has a three-dimensional character. For some purposes a one or two-dimensional approach may be sufficient, but in many problems, such as the flow through a curved river section, the three-dimensionality cannot be ignored.

In the past many efforts have been made to understand and predict the flow pattern in curved rivers. As early as 1868 Boussinesq[1] gave a mathematical description of the velocity-components in a very simple case of curved laminar flow, giving a good impression of one of the most striking features of curved shear flow, viz. the existence of a secondary circulation, clockwise if the bend turns to the left and counterclockwise if the bend turns to the right.

Afterwards, many authors have attempted to describe the steady curved shear flow mathematically, but they all had to make severe restrictions in order to solve the mathematical problems. A review of this literature is given in ref. 2.

Most investigators assume axial symmetry of the flow pattern (i.e. in each cross-section the flow field is the same), yielding a very limited class of solutions. Experiments have shown that the validity of this assumption is doubtful, at least for bends of limited turning angles.

In 1973, Kuipers and Vreugdenhil[3] attempted to attack the problem by computing the depth-averaged flow pattern in shallow curved channels, neglecting the influence of the secondary circulation but avoiding the assumption of axial symmetry. Unfortunately, their results were influenced by the computational procedure (artificial viscosity, the fitting of the curved walls in a rectangular mesh).

Recently, Engelund[10] used a greatly simplified, but non-axisymmetrical method for the computation of the flow field in

order to predict the bed configuration in a sinusoidal bend with an erodible bed. The results agree well with experimental observations.

In the present report, the secondary flow theories are extended to non-axisymmetrical flows and combined with depth-averaged computation methods. A basic assumption in this theory is that the depth of flow is much smaller than the channel width and a characteristic radius of curvature of the flow.

II. THE MATHEMATICAL MODEL

1. Coordinate-system

A Cartesian coordinate-system (x,y,z) is adopted, in which x and y are horizontal coordinates and z represents the vertical coordinate, increasing in upward direction (cf. sketch).

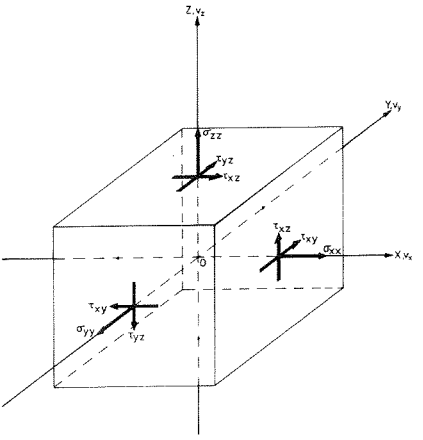

Definition sketch

A curvilinear coordinate-system may be preferable for the actual application of the method, but the essential reasoning is not influenced thereby.

2. Differential equations

If g represents the acceleration due to gravity, ρ the mass density of the fluid, v_x, v_y and v_z the velocity-components in the relevant coordinate directions and σ_{xx}, σ_{yy}, σ_{zz}, τ_{xy}, τ_{xz} and τ_{yz} the components of the stress tensor, the differential equations describing the conservation of mass and momentum in an elementary volume read:

$$\frac{\partial v_x}{\partial x} + \frac{\partial v_y}{\partial y} + \frac{\partial v_z}{\partial z} = 0 \qquad (1)$$

$$\frac{\partial (v_x^2)}{\partial x} + \frac{\partial (v_x v_y)}{\partial y} + \frac{\partial (v_x v_z)}{\partial z} = \frac{1}{\rho}\left[\frac{\partial \sigma_{xx}}{\partial x} + \frac{\partial \tau_{xy}}{\partial y} + \frac{\partial \tau_{xz}}{\partial z}\right] \qquad (2)$$

$$\frac{\partial (v_x v_y)}{\partial x} + \frac{\partial (v_y^2)}{\partial y} + \frac{\partial (v_y v_z)}{\partial z} = \frac{1}{\rho}\left[\frac{\partial \tau_{xy}}{\partial x} + \frac{\partial \sigma_{yy}}{\partial y} + \frac{\partial \tau_{yz}}{\partial z}\right] \qquad (3)$$

$$\frac{\partial (v_x v_z)}{\partial x} + \frac{\partial (v_y v_z)}{\partial y} + \frac{\partial (v_z^2)}{\partial z} = \frac{1}{\rho}\left[\frac{\partial \tau_{xz}}{\partial x} + \frac{\partial \tau_{yz}}{\partial y} + \frac{\partial \sigma_{zz}}{\partial z}\right] - g \qquad (4)$$

If the anisotropic part of the stress tensor is assumed to be related to the rate-of-strain tensor through a scalar viscosity-coefficient A(x,y,z), the components of the stress tensor can be written as:

$$\sigma_{xx} = - p + 2A \frac{\partial v_x}{\partial x} \tag{5}$$

$$\sigma_{yy} = - p + 2A \frac{\partial v_y}{\partial y} \tag{6}$$

$$\sigma_{zz} = - p + 2A \frac{\partial v_z}{\partial z} \tag{7}$$

$$\tau_{xy} = A\left(\frac{\partial v_x}{\partial y} + \frac{\partial v_y}{\partial x}\right) \tag{8}$$

$$\tau_{xz} = A\left(\frac{\partial v_x}{\partial z} + \frac{\partial v_z}{\partial x}\right) \tag{9}$$

$$\tau_{yz} = A\left(\frac{\partial v_y}{\partial z} + \frac{\partial v_z}{\partial y}\right) \tag{10}$$

where p denotes the isotropic part of the stress. The viscosity-coefficient needs further specification. This will be discussed in chapter V. Substitution of the above expressions into the balance-equations yields:

$$\frac{\partial v_x}{\partial x} + \frac{\partial v_y}{\partial y} + \frac{\partial v_z}{\partial z} = 0 \tag{1}$$

$$\frac{\partial (v_x^2)}{\partial x} + \frac{\partial (v_x v_y)}{\partial y} + \frac{\partial (v_x v_z)}{\partial z} = - \frac{1}{\rho} \frac{\partial p}{\partial x} + \frac{A}{\rho} \left[\frac{\partial^2 v_x}{\partial x^2} + \frac{\partial^2 v_x}{\partial y^2} + \frac{\partial^2 v_x}{\partial z^2}\right] +$$

$$+ \frac{1}{\rho} \left[2 \frac{\partial A}{\partial x} \frac{\partial v_x}{\partial x} + \frac{\partial A}{\partial y} \left(\frac{\partial v_x}{\partial y} + \frac{\partial v_y}{\partial x}\right) + \frac{\partial A}{\partial z} \left(\frac{\partial v_x}{\partial z} + \frac{\partial v_z}{\partial x}\right)\right] \tag{11}$$

$$\frac{\partial(v_x v_y)}{\partial x} + \frac{\partial(v_y^2)}{\partial y} + \frac{\partial(v_y v_z)}{\partial z} = -\frac{1}{\rho}\frac{\partial p}{\partial y} + \frac{A}{\rho}\left[\frac{\partial^2 v_y}{\partial x^2} + \frac{\partial^2 v_y}{\partial y^2} + \frac{\partial^2 v_y}{\partial z^2}\right] +$$

$$+ \frac{1}{\rho}\left[\frac{\partial A}{\partial x}\left(\frac{\partial v_y}{\partial x} + \frac{\partial v_x}{\partial y}\right) + 2\frac{\partial A}{\partial y}\frac{\partial v_y}{\partial y} + \frac{\partial A}{\partial z}\left(\frac{\partial v_y}{\partial z} + \frac{\partial v_z}{\partial y}\right)\right] \qquad (12)$$

$$\frac{\partial(v_x v_z)}{\partial x} + \frac{\partial(v_y v_z)}{\partial y} + \frac{\partial(v_z^2)}{\partial z} = -\frac{1}{\rho}\frac{\partial p}{\partial z} - g + \frac{A}{\rho}\left[\frac{\partial^2 v_z}{\partial x^2} + \frac{\partial^2 v_z}{\partial y^2} + \frac{\partial^2 v_z}{\partial z^2}\right] +$$

$$+ \frac{1}{\rho}\left[\frac{\partial A}{\partial x}\left(\frac{\partial v_x}{\partial z} + \frac{\partial v_z}{\partial x}\right) + \frac{\partial A}{\partial y}\left(\frac{\partial v_y}{\partial z} + \frac{\partial v_z}{\partial y}\right) + 2\frac{\partial A}{\partial z}\frac{\partial v_z}{\partial z}\right] \qquad (13)$$

3. Boundary conditions

The solution of this system must satisfy three kinds of boundary conditions:

- inflow and outflow conditions
- conditions at fixed walls (banks, bed)
- conditions at the free surface

The inflow and outflow conditions may differ from case to case, but the boundary conditions at the fixed walls and at the free surface will have the same character for all problems considered.
At a fixed wall the boundary conditions stem from the impermeability of the wall (forcing the normal velocity to vanish) and the no-slip condition (implying vanishing tangential velocity). Consequently:

$$v_x = v_y = v_z = 0 \qquad (14)$$

at the fixed walls.
At the free surface, $z = z_s(x,y)$, the boundary conditions arise from the kinematical condition of zero normal velocity and the dynamical conditions of zero pressure and tangential shear stress, yielding:

$$v_z = v_x \frac{\partial z_s}{\partial z} + v_y \frac{\partial z_s}{\partial y} \tag{15}$$

$$p = 0 \tag{16}$$

$$A\left(\frac{\partial v_x}{\partial z} + \frac{\partial v_z}{\partial x}\right) = A\left(\frac{\partial v_y}{\partial z} + \frac{\partial v_z}{\partial y}\right) = 0 \tag{17}$$

III. NORMALIZATION

Since the present mathematical model is too complex to be solved completely, it is simplified. Looking for the dominant terms in the differential equations , a normalization is carried out, such that each term of the differential equations and the boundary conditions is written as the product of a constant scale-factor and a variable (dimensionless) quantity of the order of magnitude $O(1)$*). Doing so, the importance of a term is indicated by the relative magnitude of its scale factor.
It is assumed that this normalization of the mathematical model can be realized by adopting an adequate scale-factor for each variable, either dependent or independent. So if a function f of the independent variable x may be normalized as:

$$f = F * f(x) \quad \text{while } x = X * x$$

F and X being constant scale-factors, then:

$$\frac{df}{dx} = \frac{F}{X}\frac{df}{dx} \qquad \text{with } \frac{df}{dx} = O(1)$$

In general terms, the normalization is carried out by defining:

$$x = X\xi \; ; \; y = Y\eta \; ; \; z = Z\zeta$$

$$v_x = U\,u \; ; \; v_y = V\,v \; ; \; v_z = W\,w \tag{18}$$

$$p + \rho gz = P\,p \; ; \; A = \underline{A}\,\alpha$$

*) In the sense of Landau's O-symbol: a quantity f is of the order of magnitude $O(\varepsilon^n)$ if $\lim_{\varepsilon \downarrow o} \frac{f}{\varepsilon^n}$ exists.

yielding the normalized differential equations:

$$\frac{\partial u}{\partial \xi} + \frac{VX}{UY}\frac{\partial v}{\partial \eta} + \frac{WX}{UZ}\frac{\partial w}{\partial \zeta} = 0 \qquad (19)$$

$$\frac{\partial}{\partial \xi}(u^2) + \frac{VX}{UY}\frac{\partial}{\partial \eta}(vu) + \frac{WX}{UZ}\frac{\partial}{\partial \zeta}(wu) = -\frac{P}{\rho U^2}\frac{\partial p}{\partial \xi} + \frac{A}{\rho UX} \cdot$$

$$\left[\alpha\left\{\frac{\partial^2 u}{\partial \xi^2} + \frac{X^2}{Y^2}\frac{\partial^2 u}{\partial \eta^2} + \frac{X^2}{Z^2}\frac{\partial^2 u}{\partial \zeta^2}\right\} + 2\frac{\partial \alpha}{\partial \xi}\frac{\partial u}{\partial \xi} + \frac{\partial \alpha}{\partial \eta}\left(\frac{X^2}{Y^2}\frac{\partial u}{\partial \eta} + \frac{VX}{UY}\frac{\partial v}{\partial \xi}\right) +\right.$$

$$\left. + \frac{\partial \alpha}{\partial \zeta}\left(\frac{X^2}{Z^2}\frac{\partial u}{\partial \zeta} + \frac{WX}{UZ}\frac{\partial w}{\partial \xi}\right)\right] \qquad (20)$$

and two other momentum-equations.

In this way the problem of estimating the order of magnitude of the terms in the differential equations has been "translated" into the problem of choosing the correct scale-factors of the variables. In essence both problems are similar, but the latter provides a more systematical attack.

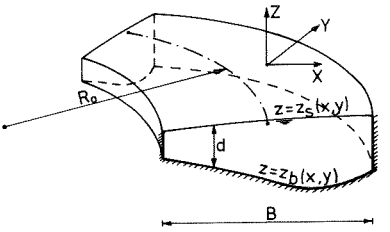

The actual choice of the scale-factors is based on the following considerations (see sketch):

1. The horizontal coordinates have not yet been related to the channel geometry and therefore the coordinates x and y as well as the velocity-components v_x and v_y must be equivalent in the equations. Hence:

$$X = Y \quad \text{and} \quad U = V$$

2. In a shallow river at large distances from the banks (say at least a few times the average depth of flow), the shear stress terms in the momentum-equations including derivatives with respect to z will be predominant. So restricting the problem to shallow rivers, one can state:

$$\frac{X^2}{Z^2} >> 1$$

3. In the case mentioned above, the vertical derivative of the main velocity-component is estimated to be:

$$\frac{\partial v_{tot}}{\partial z} = \frac{\bar{v}_{tot}}{d} O(1)$$

in which $\bar{v}_{tot}$ = the depth-averaged value of v_{tot} and d = depth of flow. Therefore the scale-factors of the vertical coordinate and the horizontal velocity-components are chosen as:

$$U = V = \frac{Q}{B\,\underline{d}} \quad ; \quad Z = \underline{d} \tag{21}$$

in which: Q = total discharge
B = representative channel-width
$\underline{d}$ = characteristic depth of flow (for instance the overall mean value)

4. The deviation from uniform flow is caused by the curvature of the channel and the configuration of the bed. A characteristic radius of curvature, such as the average radius of curvature R_0 of the channel axis, will be an adequate scale-factor for the horizontal coordinates if the influence of the bed configuration is not dominant. Then:

$$X = Y = R_0 \tag{22}$$

Otherwise the horizontal length scale must be based on the bed configuration.

5. In the equation of continuity, the term including $\frac{\partial w}{\partial \zeta}$ can not be expected to be dominant over the other terms. So at most:

$$\frac{WX}{UZ} = 1 \text{ or, taking account of 21 and 22:}$$

$$W = \frac{d}{R_0} V \tag{23}$$

6. The normalized model must include the case of uniform, rectilinear shear flow, for instance along the x-axis. For $X = Y = R_0$ eq. 20 then reduces to:

$$0 = - \frac{P}{\rho V^2} \frac{\partial p}{\partial \xi} + \frac{A}{\rho UX} \frac{X^2}{Z^2} \frac{\partial}{\partial \zeta} \left(\alpha \frac{\partial u}{\partial \zeta}\right) \tag{24}$$

Since both terms in this equation must be of the same order of magnitude, one can state:

$$\frac{P}{\rho V^2} = \frac{A}{\rho UX} \frac{X^2}{Z^2} \text{ or, regarding 21 and 22:}$$

$$P = \rho V^2 \frac{R_0}{d} (Re')^{-1} \tag{25}$$

where $Re' = \frac{\rho V \underline{d}}{\underline{A}}$ can be considered as a scale-factor for the Reynolds number based on the turbulent viscosity and the depth of flow.
As an alternative, P could be defined proportional to $\rho g \underline{d}$ (the pressure will be nearly hydrostatic). In that case eq. 24 yields:

$$P = \rho g \underline{d} \frac{V^2}{g \underline{d}} \frac{R_0}{\underline{d}} \frac{1}{Re'} \qquad (26)$$

So $P = \rho g d$ is applicable to the present problem if

$$\frac{V^2}{g \underline{d}} \frac{R_0}{\underline{d}\, Re'} = 0_s(1)^{*)}$$

7. The Reynolds number scale Re' is a very important factor in the normalized momentum-equations. If Re' is of the order 0(1), the friction terms dominate the inertial terms. In that case a first approximation of the velocity field can be based on friction, piezometric head and continuity.
If $1/Re' = 0(\frac{\underline{d}}{R_0})$, however, friction terms and inertial terms are equally important and then the latter terms can no longer be neglected, not even in a first approximation.
As a consequence, the Reynolds number scale has great influence on the method of solution of the problem.

---

*) In the sense of Landau's 0_s-symbol: a quantity is of the order of magnitude $0_s(\varepsilon^n)$ if $\lim_{\varepsilon \downarrow o} \frac{f}{\varepsilon^n}$ exists and $\neq 0$.

At this point the friction is assumed to be dominant, so $Re' = 1$.

In chapter IX, the consequences of this assumption for the applicability of the solution will receive further attention.

According to (25) P may then be chosen as:

$$P = \frac{\rho V^2 R_0}{\underline{d}} \tag{27}$$

The scale-factors defined by defs. 21-27 are substituted into the system of differential equations and boundary conditions. Defining ε by $\underline{d}/R_0$, whence $\varepsilon << 1$, the normalized system is found to read:

$$\frac{\partial u}{\partial \xi} + \frac{\partial v}{\partial \eta} + \frac{\partial w}{\partial \zeta} = 0 \tag{28}$$

$$\varepsilon\{\frac{\partial}{\partial \xi}(u^2) + \frac{\partial}{\partial \eta}(uv) + \frac{\partial}{\partial \zeta}(uw)\} = -\frac{\partial p}{\partial \xi} + \alpha\{\frac{\partial^2 u}{\partial \zeta^2} + \varepsilon^2 \frac{\partial^2 u}{\partial \eta^2} +$$

$$+ \varepsilon^2 \frac{\partial^2 u}{\partial \xi^2}\} + 2\varepsilon^2 \frac{\partial \alpha}{\partial \xi}\frac{\partial u}{\partial \xi} + \varepsilon^2 \frac{\partial \alpha}{\partial \eta}(\frac{\partial u}{\partial \eta} + \frac{\partial v}{\partial \xi}) +$$

$$+ \frac{\partial \alpha}{\partial \zeta}(\frac{\partial u}{\partial \zeta} + \varepsilon^2 \frac{\partial w}{\partial \xi}) \tag{29}$$

$$\varepsilon\{\frac{\partial}{\partial \xi}(uv) + \frac{\partial}{\partial \eta}(v^2) + \frac{\partial}{\partial \zeta}(vw)\} = -\frac{\partial p}{\partial \eta} + \alpha\{\frac{\partial^2 v}{\partial \zeta^2} + \varepsilon^2 \frac{\partial^2 v}{\partial \eta^2} +$$

$$+ \varepsilon^2 \frac{\partial^2 v}{\partial \xi^2}\} + \varepsilon^2 \frac{\partial \alpha}{\partial \xi}(\frac{\partial v}{\partial \xi} + \frac{\partial u}{\partial \eta}) + 2\varepsilon^2 \frac{\partial \alpha}{\partial \eta}\frac{\partial v}{\partial \eta} +$$

$$+ \frac{\partial \alpha}{\partial \zeta}(\frac{\partial v}{\partial \zeta} + \varepsilon^2 \frac{\partial w}{\partial \eta}) \tag{30}$$

$$\varepsilon^2 \{\frac{\partial}{\partial \xi}(uw) + \frac{\partial}{\partial \eta}(vw) + \frac{\partial}{\partial \zeta}(w^2)\} = -\frac{\partial p}{\partial \zeta} + \varepsilon^2 \alpha\{\frac{\partial^2 w}{\partial \zeta^2} + \varepsilon^2 \frac{\partial^2 w}{\partial \eta^2} +$$

$$+ \varepsilon^2 \frac{\partial^2 w}{\partial \xi^2}\} + \varepsilon^2\{\frac{\partial \alpha}{\partial \xi}(\varepsilon^2 \frac{\partial w}{\partial \xi} + \frac{\partial u}{\partial \zeta}) + \frac{\partial \alpha}{\partial \eta}(\varepsilon^2 \frac{\partial w}{\partial \eta} + \frac{\partial v}{\partial \zeta}) +$$

$$+ 2 \frac{\partial \alpha}{\partial \zeta} \frac{\partial w}{\partial \zeta}\} \qquad (31)$$

with the boundary conditions:

- at the fixed walls (bed and banks): $u = v = w = 0$ (32)

- at the free surface $\zeta = \zeta_s$: $w = u\frac{\partial \zeta_s}{\partial \xi} + v\frac{\partial \zeta_s}{\partial \eta}$ (33)

$$p = \frac{g\underline{d}}{V^2}\varepsilon\zeta_s \qquad (34)$$

$$\alpha(\frac{\partial u}{\partial \zeta} + \varepsilon^2 \frac{\partial w}{\partial \xi}) = \alpha(\frac{\partial v}{\partial \zeta} + \varepsilon^2 \frac{\partial w}{\partial \eta}) = 0 \qquad (35)$$

Condition 34 shows that p is of the order $0_s(1)$ at the free surface if $\frac{g\underline{d}}{V^2} = 0_s(1)$. In that case, according to eq. 26, $P = \rho g\underline{d}$ is applicable as well.

Summary of restrictions

The present normalization restricts the applicability of the mathematical model at the following points:

- the channel must be shallow, but not necessarily of uniform cross-section.
- the characteristic depth of flow must be small with respect to the horizontal length scale.

- if a characteristic radius of curvature of the channel is chosen as a horizontal length scale, the influence of the bed configuration on the flow field must not dominate the influence of the channel curvature. Otherwise, the horizontal length scale must be based on the bed configuration.
- the shear stress effects must dominate the inertial effects ($Re' = O(1)$).

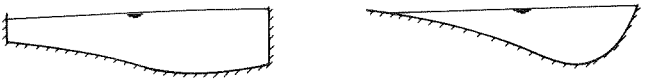

Included in the normalized model
(except the bank regions).

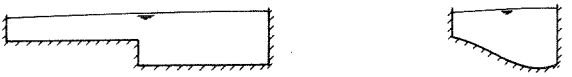

Not included in the normalized model.

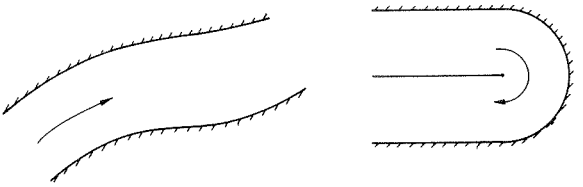

Included Not included

IV. METHOD OF SOLUTION

The normalized problem will be attacked by means of a well-known method of regular asymptotic expansions. If $f(\xi,\eta,\zeta,\varepsilon')$ denotes any dependent variable of the normalized system, ε' being a small parameter, it is attempted to find a solution of f of the form:

$$f(\xi,\eta,\zeta;\varepsilon') = \sum_{i=o}^{\infty} (\varepsilon')^i f_i (\xi,\eta,\zeta;\varepsilon') \text{ with } f_i = O(1) \quad (36)$$

Each function f_i (called here the (i)th order subfunction of f) is solved from the corresponding approximation of the differential equations and the boundary conditions, starting from i=0 and going on with i=1,2,3,....., successively.

The small geometrical parameter $\varepsilon = \underline{d}/R_0$ is selected as the perturbation parameter here, since it represents the curved character of the flow.

The convergence of the power series expansions according to (36) will not be considered, since this may be expected to raise very complicated mathematical problems which are far beyond the scope of the present report. In order to obtain a rough indication of the limitations of the solution, however, it will be checked whether the consecutive terms in the expansions decrease, if at least the subfunctions in these terms have been determined.

Algorithm to the asymptotic solution of the system.

1. Expand each of the dependent variables u, v, w, p and α in a power series of ε, according to 36 and substitute these expansions into the normalized differential equations 28 through 31 and the boundary conditions 32 through 35.

2. Collect all terms of the order of magnitude O(1) in each equation and neglect all smaller terms. This yields the so-called zero order differential equations.
3. Determine the boundary conditions of the zero order system (see Appendix I).
4. Solve the zero order system.
5. Eliminate all terms O(1) from the complete equations resulting from 1., collect all terms of the order of magnitude $O(\varepsilon)$ in each equation and neglect all smaller terms. This yields the first order equations.
6. Determine the boundary conditions of the first order system (App. I).
7. Solve the first order system.

Repeat steps 5 through 7 for successively higher powers of ε.

An important feature of this asymptotic method is the possibility that not all boundary conditions can be satisfied. In the present case all inertia terms as well as the greater part of the stress terms vanish from the zero order equations. As a consequence, the only boundary condition which can be satisfied at the banks is the condition of impermeability to the main flow, which provides the lateral bounds of the main flow. The no-slip conditions at the banks are not satisfied, so the solution must be expected to hold good only at some distance from the banks, where the latter conditions have ceased to influence the flow pattern. This emphasizes again that the solution is only applicable to shallow flows.

V. TURBULENCE MODEL AND BOUNDARY CONDITIONS AT THE BED

In turbulent flows, the shear stresses appearing in the momentum-equations (2-4) consist of two parts, one of which arises from the molecular viscosity, while the other one represents the exchange of momentum due to turbulence. Therefore, if the shear stress is assumed to be proportional to the rate of strain (eqs. 5-10), the coefficient of proportionality consists of two parts:

$$A = \rho\nu + A_t(x,y,z) \tag{37}$$

in which ν denotes the kinematical viscosity of the fluid and $A_{t(urbulence)}$ is called eddy viscosity or coefficient of turbulence viscosity. In general, A_t depends on the velocity field, so on the solution of the mathematical problem, which itself depends on A_t again. Consequently, the mathematical problem does not form a closed system in case of turbulent flow.

The most usual way to make the system closed is to assume a distribution of A_t over the flow field or to prescribe its dependence on the velocity field. The latter will be done here and to that end some simplifying assumptions will be made:

1. The molecular part of the viscosity can be neglected with respect to the turbulent part. So:

$$\rho\nu \ll A_t \quad \text{or} \quad \frac{\nu}{Vd} \ll \alpha_t \tag{38}$$

2. At any point of the flow field the turbulence effects in the vertical direction are the most important. This is in accordance with the earlier assumption of shallow

channels. It implies that in a first approximation the main flow can be considered as a simple shear flow in a (horizontally curved) vertical surface.

3. A mixing-length hypotheses can be used to describe the eddy viscosity:

$$\alpha_t = L^2\{(\frac{\partial u}{\partial \zeta})^2 + (\frac{\partial v}{\partial \zeta})^2\}^{\frac{1}{2}} \qquad (39)$$

This is a rather crude assumption, presumably adequate to a first approximation of the main flow, but at the least questionable for more complex flow fields like the present one, where the curvature and the secondary flow will influence the turbulence (Bradshaw[4]).

Nevertheless, a mixing-length hypothesis is adopted because:

- it allows for a rather simple solution, whereas more advanced turbulence models (Launder and Spalding[5]) do not. So it may be interesting to find out to what extent this simple approach yields results which are applicable in engineering practice.
- many authors dealing with axisymmetric curved river flow have made assumptions as to the turbulent shear stress which are based on a mixing-length hypothesis (Rozovskii[6]) or could be derived from it. It may be interesting to compare the results for axisymmetric flow with the results of a similar theory for an actual bend.

B.C. Yen[7] corrects α_t for curvature effects in the following way:

$$\alpha_t = L^2\{(\frac{\partial u}{\partial \zeta})^2 + (\frac{\partial v}{\partial \zeta})^2\}^{\frac{1}{2}} F(r) \qquad (40)$$

where r denotes some quantity indicating the curvature of the main flow. F is chosen such that the average lateral dispersion coefficient is proportional to $1/r^2$. From a physical point of view this is a rather weak basis, whence F is set equal to 1 here.

4. Rozovskii concluded from experiments that throughout the bend the vertical distribution of the main velocity-component far from the banks remains close to the well-known logarithmic distribution of uniform shear flow. Besides he showed for axisymmetric curved flows that the transverse velocity-component agrees better with experimental results when computed from a logarithmic main flow than when computed from any other distribution (parabolic, power law, elliptic).
Therefore, an expression of L will be adopted that is known to generate the logarithmic distribution in case of uniform flow:

$$L = \kappa(\zeta - \zeta_b)\left(\frac{\zeta_s - \zeta}{\zeta_s - \zeta_b}\right)^{\frac{1}{2}} \qquad (41)$$

where κ = Von Kármán's constant, ζ_s = normalized free surface level, ζ_b = normalized bed level.
Excluding the correction factor for curvature effects, the expression of α_t finally becomes:

$$\alpha_t = -\kappa^2 \frac{\zeta - \zeta_s}{\zeta_s - \zeta_b}(\zeta - \zeta_b)^2 \left\{\left(\frac{\partial u}{\partial \zeta}\right)^2 + \left(\frac{\partial v}{\partial \zeta}\right)^2\right\}^{\frac{1}{2}} \qquad (42)$$

The power series expansion of this expression is given in Appendix II.

A problem arising from the logarithmic distribution is how to account for the no-slip condition at the bed, where the logarithm has no finite value. In uniform flow theory it is usual to cope with this problem by prescribing the level where the logarithm equals zero. This level lies somewhat above the bed, say at $\zeta = \zeta_b + \zeta'$. Then the expression for the velocity distribution reads:

$$u = \frac{1}{\kappa} \sqrt{(\zeta_s - \zeta_b)\, I}\ \ln\left(\frac{\zeta - \zeta_b}{\zeta'}\right) \tag{43}$$

where I is the slope of the energy-line. Then:

$$\bar{u} \approx \frac{1}{\zeta_s - \zeta_b} \int_{\zeta_b + \zeta'}^{\zeta_s} u\, d\zeta = \frac{1}{\kappa} \sqrt{(\zeta_s - \zeta_b)\, I}\ \{-1 + \zeta' - \ln\zeta' + \ln(\zeta_s - \zeta_b)\} \tag{44}$$

Adopting Chezy's law for shallow flows:

$$\bar{u} = \frac{C}{\sqrt{g}} \sqrt{(\zeta_s - \zeta_b)\, I} \tag{45}$$

where C denotes Chezy's constant, and equating 44 and 45 yields for

$\zeta' << |\ln \zeta'|$:

$$\zeta' = \exp\{-1 - \frac{\kappa C}{\sqrt{g}} + \ln(\zeta_s - \zeta_b)\} \tag{46}$$

Then the expression for the velocity-distribution can be written as:

$$u = \bar{u}\ \{1 + \frac{\sqrt{g}}{\kappa C} + \frac{\sqrt{g}}{\kappa C} \ln\left(\frac{\zeta - \zeta_b}{\zeta_s - \zeta_b}\right)\} \tag{47}$$

A graphical representation of this distribution is given in fig. 1.
Correspondingly, in case of curved flow the original no-slip conditions at the bed are replaced by:

$$u(\zeta = \zeta_b + \zeta') = v(\zeta = \zeta_b + \zeta') = 0 \qquad (48)$$

where ζ' follows from eq. 46.

This assumption may be plausible for a first approximation of the main flow. For the secondary flow it is doubtful, as it would imply that the transverse velocity profile (which will contain logarithm-like functions as well) becomes zero at the same, artificially introduced level as the main flow profile. Besides it is unlikely that Chezy's constant will determine that level.
Considering other authors, one finds several types of boundary conditions at or close to the bed.

1. For smooth beds, Rozovskii[6] supposes the transverse shear stress to vanish at the bed instead of the transverse velocity. He arrives at this condition by the following considerations (for axisymmetric shallow flows far from the banks):
   - there must be a point at some distance δ above the bed where the vertical gradient of the transverse velocity-component (and consequently the transverse shear stress) equals zero (see sketch).
     The momentum balance in the layer below this level shows that the transverse bed shear stress is of the order of magnitude $O(\delta/d)$. For smooth beds δ is small with respect to the depth of flow.

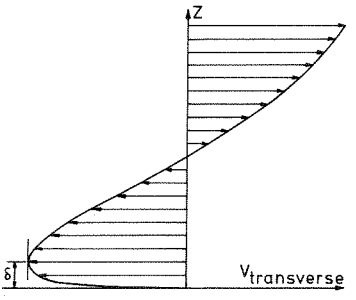

- in the shallow water approximation, the piezometric head is nearly constant in a vertical. Therefore the gradient of the piezometric head is proportional to the slope of the free surface.
- averaging the transverse equation of motion over the depth of flow shows that the transverse slope of the free surface consists of two components, one caused by the average centrifugal force and the other one caused by the radial bed shear stress. In case of a smooth bed, the latter component can be neglected with respect to the former one, since it is of the order $O(\delta/d)$.
- the slope term in the transverse equation of motion can be approximated as above. This is equivalent to setting the radial bed shear stress equal to zero.

In chapter VII it will be shown that the transverse velocity profile near the bed, satisfying condition 48, can differ considerably from the profile based on Rozovskii's condition, even though in both cases the transverse bed

shear stress is negligible with respect to the centrifugal effect.

2. Ananyan[8] uses the laminar sublayer concept, assuming the thickness of the sublayer to be the same as in a uniform flow with the same shear velocity. The results of this approach turn out to be very similar to those obtained by condition 48. Condition 48 is simpler, however and therefore preferable.

3. Kikkawa et al.[9] state that a turbulent boundary layer must develop from the outer wall towards the inner wall as a consequence of the secondary flow. The thickness of this layer, δ, is defined as the vertical distance from the bed to the level where the transverse velocity has a zero gradient (see sketch).

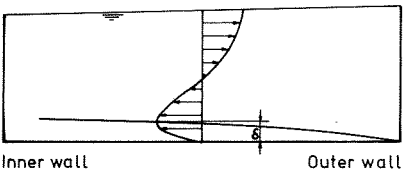

As mentioned above, the transverse shear stress equals zero at the edge of this layer. Therefore, the momentum balance in the boundary layer provides an expression for the bed shear stress, which does not depend on the transverse velocity profile as long as the transverse slope of the free surface can be approximated by the centrifugal effect alone. As stated above, this is only true for smooth beds.

In addition, expressions are given for the boundary layer

thickness and the transverse shear velocity as functions of the fluid viscosity, the channel width and the local transverse velocity at the edge of the boundary layer. These expressions are derived from the theory of the developing boundary layer at a smooth flat plate. Together with the formula for the transverse bed shear stress they provide an explicit expression for the boundary layer thickness. It is questionable whether this condition can be applied to a rough bed, as the authors suppose. Even if it is limited to smooth beds, an important objection is, that the layer between the level δ and the bed is essentially different from the boundary layer at a smooth flat plate. Hence the flat plate theory for the growth of the layer can not be transferred to this problem.

4. A very widely applied rough bed condition is given by Rozovskii[6], who states that the shear stress vector close the bed must coincide with the velocity-vector there, since the force exerted by the bed upon the stream is not primarily determined by viscous effects, but by the presence of roughness elements obstructing the stream near the bed. This is essentially different from the smooth bed, where the force arises entirely from viscous effects. Then the shear stress vector can deviate from the velocity-vector close to the bed. From this point of view condition 48 should be considered as a smooth bed condition.
Rozovskii's condition seems to have a sound physical basis, but it raises another question: at what level must the condition be imposed?
Without further arguments Rozovskii takes the equivalent bottom roughness k as the distance from this level to the bed, while k is assumed to be related to Chezy's constant

in the same way as in uniform flow. This could be reasonable, supposing the flow very near the bed behaves like a uniform flow with the same bed shear stress. From this point of view condition 48 can be defended as well, since in uniform flow it is applicable both in smooth and in rough bed cases.

Moreover, using Rozovskii's condition the solution of the mathematical problem is only fully determined in axisymmetric flows. Otherwise an additional condition is needed near the bed, as will be shown in chapter VI.

For instance, this could be a prescription of the level where the total velocity equals zero or of the value of the total velocity at a distance k above the bed.

An essentially different approach to both the turbulence model and the boundary condition at the bed is suggested by Engelund[10], who assumes that the eddy viscosity is constant in a vertical, introducing a slip-velocity at the bed. Consequently, the main flow profile is the well-known Boussinesq-Bazin parabola (fig. 1). For the secondary flow Engelund uses the aforementioned rough bed condition, which is sufficient as he assumes the transverse velocity to have the same vertical distribution everywhere in the flow field (then the solution procedure is the same as in the axisymmetrical case).

Ananyan[8] and Ikeda[11] suggest some kind of mixture between the logarithmic and the parabolic law, adopting a logarithmic main flow distribution, but a constant eddy viscosity when computing the secondary flow.

Finally, Rozovskii[6] studied several other main flow distributions (power law, elliptic), but even though they are rather good approximations to the main flow, they turned out to yield secondary flow profiles which were inferior to those obtained

from the logarithmic profile. Therefore they will not receive further attention.

In chapter VII the results of the present model and of the most important other models mentioned will be compared to one another and to experimental results.
First, the next chapter gives a description of the solution procedure.

VI. SOLUTION IN CASE OF PREDOMINANT SHEAR STRESS

Since the essential points of the solution procedure are hardly influenced by the turbulence models mentioned in chapter V, the present model is maintained here.

1. Zero order system

Applying the solution algorithm to eqs. 28 through 35 yields the following zero order system:

$$\frac{\partial u_0}{\partial \xi} + \frac{\partial v_0}{\partial \eta} + \frac{\partial w_0}{\partial \zeta} = 0 \tag{49}$$

$$0 = - \frac{\partial p_0}{\partial \xi} + \frac{\partial}{\partial \zeta} \left(\alpha_0 \frac{\partial u_0}{\partial \zeta} \right) \tag{50}$$

$$0 = - \frac{\partial p_0}{\partial \eta} + \frac{\partial}{\partial \zeta} \left(\alpha_0 \frac{\partial v_0}{\partial \zeta} \right) \tag{51}$$

$$0 = - \frac{\partial p_0}{\partial \zeta} \tag{52}$$

$$u_0 \big|_{\zeta_b + \zeta_0'} = v_0 \big|_{\zeta_b + \zeta_0'} = w_0 \big|_{\zeta_b + \zeta_0'} = 0 \tag{53}^*$$

$$\left(\alpha_0 \frac{\partial u_0}{\partial \zeta} \right) \big|_{\zeta_{s0}} = \left(\alpha_0 \frac{\partial v_0}{\partial \zeta} \right) \big|_{\zeta_{s0}} = 0 \tag{54}$$

$$w_0 \big|_{\zeta_{s0}} = \left(u_0 \frac{\partial \zeta_{s0}}{\zeta \xi} + v_0 \frac{\partial \zeta_{s0}}{\partial \eta} \right) \big|_{\zeta_{s0}} \tag{55}^*$$

*) Solving w_0 from eq. 49, only one boundary condition is needed. Cond. 55 is preferable here, as all free surface boundary conditions are imposed at one well-defined level, whereas it is not certain whether the condition for w_0 should be imposed at $\zeta = \zeta_b$ or at $\zeta = \zeta_b + \zeta_0'$.

$$p_0|_{\zeta_{s0}} = \frac{\zeta_{s0}}{F^2} \tag{56}$$

in which:

$$\zeta_0' = \exp\{-1 - \frac{\kappa C}{\sqrt{g}} + \ln(\zeta_{s0} - \zeta_b)\} \tag{57}$$

and:

$$\frac{1}{F^2} = \frac{\varepsilon g d}{V^2} \tag{58}$$

In order to solve the zero order system, it is assumed that the shape of the vertical distribution of the main velocity is constant throughout the flow field. This is in accordance with the conception of the main flow being a curved version of uniform flow, adopted in the foregoing chapters.
Eqs. 50 and 51 show that u_0 and v_0 may be considered as the zero order components of this main flow. Hence their vertical distributions must be similar.
So the zero order main velocity is written as:

$$u_0' = \bar{u}_0' \, f_0(\zeta, \zeta_{s0}, \zeta_b) \tag{59}$$

and its components in the horizontal directions are:

$$u_0 = \bar{u}_0 \, f_0(\zeta, \zeta_{s0}, \zeta_b) \text{ and } v_0 = \bar{v}_0 \, f_0(\zeta, \zeta_{s0}, \zeta_b) \tag{60}$$

In these expressions, $\bar{u}_0'$, $\bar{u}_0$ and $\bar{v}_0$ denote depth-averaged quantities as defined in appendix III. Consequently:

$$\bar{f}_0 = 1 \tag{61}$$

Subsequently, the zero order system can be solved, yielding:

$$u_0 = \bar{u}_0\{1 + \frac{\sqrt{g}}{\kappa C} + \frac{\sqrt{g}}{\kappa C} \ln(1 + Z_0)\} \tag{62}$$

$$v_0 = \bar{v}_0\{1 + \frac{\sqrt{g}}{\kappa C} + \frac{\sqrt{g}}{\kappa C} \ln(1 + Z_0)\} \tag{63}$$

$$w_0 = -(\zeta_{s0} - \zeta_b)\{\frac{\partial \bar{u}_0}{\partial \xi} + \frac{\partial \bar{v}_0}{\partial \eta}\}(1 + Z_0)\{1 + \frac{\sqrt{g}}{\kappa C} + \frac{\sqrt{g}}{\kappa C} \ln(1 + Z_0)\} +$$

$$+ (\bar{u}_0 \frac{\partial \zeta_b}{\partial \xi} + \bar{v}_0 \frac{\partial \zeta_b}{\partial \eta})\{1 + \frac{\sqrt{g}}{\kappa C} + \frac{\sqrt{g}}{\kappa C} \ln(1 + Z_0)\} \tag{64}*$$

$$p_0 = \bar{p}_0 = \frac{\zeta_{s0}}{F^2} \tag{65}$$

in which:

$$Z_0 = \frac{\zeta - \zeta_{s0}}{\zeta_{s0} - \zeta_b} \tag{66}$$

The depth-averaged functions $\bar{u}_0$, $\bar{v}_0$ and $\bar{p}_0$ must be solved from the depth-averaged zero order equation of continuity:

$$\frac{1}{\zeta_{s0} - \zeta_b}\left[\frac{\partial}{\partial \xi}\{\bar{u}_0(\zeta_{s0} - \zeta_b)\} + \frac{\partial}{\partial \eta}\{\bar{v}_0(\zeta_{s0} - \zeta_b)\}\right] = \tag{67}$$

and the depth-averaged zero order equations of motion:

$$\frac{\partial \bar{p}_0}{\partial \xi} = -\frac{g}{C^2} \frac{\bar{u}_0 \bar{u}_0'}{\zeta_{s0} - \zeta_b} \tag{68}$$

---

*) This solution satisfies both cond. 53 and cond. 55, which implies that the boundary condition near the bed should be imposed at $\zeta = \zeta_b + \zeta_0'$ rather than at $\zeta = \zeta_b$.

$$\frac{\partial \bar{p}_0}{\partial \eta} = - \frac{g}{c^2} \frac{\bar{v}_0 \bar{u}_0'}{\zeta_{s0} - \zeta_b} \tag{69}$$

This solution will be discussed in chapter VIII.

2. First order system

The first order differential equations read:

$$\frac{\partial u_1}{\partial \xi} + \frac{\partial v_1}{\partial \eta} + \frac{\partial w_1}{\partial \zeta} = 0 \tag{70}$$

$$\frac{\partial (u_0^2)}{\partial \xi} + \frac{\partial (u_0 v_0)}{\partial \eta} + \frac{\partial (u_0 w_0)}{\partial \zeta} = - \frac{\partial p_1}{\partial \xi} + \frac{\partial}{\partial \zeta}(\alpha_0 \frac{\partial u_1}{\partial \zeta} + \alpha_1 \frac{\partial u_0}{\partial \zeta}) \tag{71}$$

$$\frac{\partial (u_0 v_0)}{\partial \zeta} + \frac{\partial (v_0^2)}{\partial \eta} + \frac{\partial (v_0 w_0)}{\partial \zeta} = - \frac{\partial p_1}{\partial \eta} + \frac{\partial}{\partial \zeta}(\alpha_0 \frac{\partial v_1}{\partial \zeta} + \alpha_1 \frac{\partial v_0}{\partial \zeta}) \tag{72}$$

$$0 = - \frac{\partial p_1}{\partial \zeta} \tag{73}$$

According to appendix 1, the relevant boundary conditions are:

$$u_1 \big|_{\zeta_b} + \zeta_0' = - \frac{\zeta_{s1}}{\zeta_{s0} - \zeta_b} \frac{\sqrt{g}}{\kappa C} \bar{u}_0 \tag{74}$$

$$v_1 \big|_{\zeta_b} + \zeta_0' = - \frac{\zeta_{s1}}{\zeta_{s0} - \zeta_b} \frac{\sqrt{g}}{\kappa C} \bar{v}_0 \tag{75}$$

$$w_1 \big|_{\zeta_b} + \zeta_0' = \frac{\zeta_{s1}}{\zeta_{s0} - \zeta_b} \frac{\sqrt{g}}{\kappa C} (\bar{u}_0 \frac{\partial \zeta_b}{\partial \xi} + \bar{v}_0 \frac{\partial \zeta_b}{\partial \eta}) \tag{76}$$

$$(\alpha_0 \frac{\partial u_1}{\partial \zeta} + \alpha_1 \frac{\partial u_0}{\partial \zeta}) \big|_{\zeta_{s0}} = \frac{\zeta_{s1}}{\zeta_{s0} - \zeta_b} \frac{g}{C^2} \bar{u}_0 \bar{u}_0' \tag{77}$$

$$(\alpha_0 \frac{\partial v_1}{\partial \zeta} + \alpha_1 \frac{\partial v_0}{\partial \zeta})\Big|_{\zeta_{s0}} = \frac{\zeta_{s1}}{\zeta_{s0} - \zeta_b} \frac{g}{c^2} \bar{v}_0 \bar{u}_0' \tag{78}$$

$$w_1\Big|_{\zeta_{s0}} = -\zeta_{s1}(\frac{\partial w_0}{\partial \zeta})\Big|_{\zeta_{s0}} + (u_1 \frac{\partial \zeta_{s0}}{\partial \xi} + v_1 \frac{\partial \zeta_{s0}}{\partial \eta} + u_0 \frac{\partial \zeta_{s1}}{\partial \xi} +$$

$$+ v_0 \frac{\partial \zeta_{s1}}{\partial \eta})\Big|_{\zeta_{s0}} + \zeta_{s1} (\frac{\partial u_0}{\partial \zeta} \frac{\partial \zeta_{s0}}{\partial \xi} + \frac{\partial v_0}{\partial \zeta} \frac{\partial \zeta_{s0}}{\partial \eta})\Big|_{\zeta_{s0}} \tag{79}*$$

$$p_1\Big|_{\zeta_{s0}} = \frac{\zeta_{s1}}{F^2} \tag{80}$$

The solution of this system is:

$$u_1 = \bar{u}_1\{1 + \frac{\sqrt{g}}{\kappa C} + \frac{\sqrt{g}}{\kappa C} \ln(1+Z_0)\} - \frac{\zeta_{s1}}{\zeta_{s0} - \zeta_b} \frac{\sqrt{g}}{\kappa C} \bar{u}_0 +$$

$$-(\zeta_{s0} - \zeta_b) \tilde{u}_1[2F_1(Z_0) + \frac{\sqrt{g}}{\kappa C} F_2(Z_0) - 2(1 - \frac{\sqrt{g}}{\kappa C})\{1 + \frac{\sqrt{g}}{\kappa C} + \frac{\sqrt{g}}{\kappa C} *$$

$$\ln(1+Z_0)\}] \tag{81}$$

$$v_1 = \bar{v}_1\{1 + \frac{\sqrt{g}}{\kappa C} + \frac{\sqrt{g}}{\kappa C} \ln(1+Z_0)\} - \frac{\zeta_{s1}}{\zeta_{s0} - \zeta_b} \frac{\sqrt{g}}{\kappa C} \bar{v}_0 +$$

$$-(\zeta_{s0} - \zeta_b)\tilde{v}_1[2F_1(Z_0) + \frac{\sqrt{g}}{\kappa C} F_2(Z_0) - 2(1 - \frac{\sqrt{g}}{\kappa C})\{1 + \frac{\sqrt{g}}{\kappa C} + \frac{\sqrt{g}}{\kappa C} *$$

$$\ln(1+Z_0)\}] \tag{82}$$

---

*) Only one of these conditions is needed for solving w_1.

$$p_1 = \bar{p}_1 = \frac{\zeta_{s1}}{F^2} \tag{83}$$

in which:

$$\tilde{u}_1 = \frac{1}{2\kappa^2 \bar{u}_0'^3} \{(\bar{u}_0'^2 + \bar{v}_0^2)\ \bar{T}_{\xi 0} - \bar{u}_0 \bar{v}_0\ \bar{T}_{\eta 0}\} \tag{84}$$

$$\tilde{v}_1 = \frac{1}{2\kappa^2 \bar{u}_0'^3} \{(\bar{u}_0'^2 + \bar{u}_0^2)\ \bar{T}_{\eta 0} - \bar{u}_0 \bar{v}_0\ \bar{T}_{\xi 0}\} \tag{85}$$

$$\bar{T}_{\xi 0} = \bar{u}_0 \frac{\partial \bar{u}_0}{\partial \xi} + \bar{v}_0 \frac{\partial \bar{u}_0}{\partial \eta} \tag{86}$$

$$\bar{T}_{\eta 0} = \bar{u}_0 \frac{\partial \bar{v}_0}{\partial \xi} + \bar{v}_0 \frac{\partial \bar{v}_0}{\partial \eta} \tag{87}$$

$$F_1(Z_0) = \int_{-1+Z_0'}^{Z_0} \frac{\ln(1+Z_0)}{Z_0}\, dZ_0 \tag{88}$$

$$F_2(Z_0) = \int_{-1+Z_0'}^{Z_0} \frac{\ln^2(1+Z_0)}{Z_0}\, dZ_0 \tag{89}$$

$$Z_0' = \frac{\zeta_0'}{\zeta_{s0} - \zeta_b} = \exp(-1 - \frac{\kappa C}{\sqrt{g}}) \tag{90}$$

Subsequently, w_1 can be solved from eq. 70, yielding a fairly complex expression which is not relevant to the argumentation. Therefore it will be left out.

The depth-averaged functions $\bar{u}_1$, $\bar{v}_1$ and $\bar{p}_1$ must be solved from the depth-integrated first order equation of continuity:

$$\frac{\partial}{\partial \xi}\{\bar{u}_1 (\zeta_{s0} - \zeta_b) + \bar{u}_0 \zeta_{s1}\} + \frac{\partial}{\partial \eta}\{\bar{v}_1(\zeta_{s0} - \zeta_b) + v_0 \zeta_{s1}\} = 0 \qquad (91)$$

and the depth-averaged first order equations of motion:

$$\frac{\partial \bar{p}_1}{\partial \xi} = -\frac{g}{c^2}\frac{1}{\zeta_{s0} - \zeta_b}\frac{1}{\bar{u}_0'}\{(\bar{u}_0'^2 + \bar{u}_0^2)\bar{u}_1 + \bar{u}_0\bar{v}_0\bar{v}_1\} +$$

$$+ \frac{g}{c^2}\frac{\zeta_{s1}}{(\zeta_{s0} - \zeta_b)^2}\bar{u}_0'\bar{u}_0 - (1+3\frac{g}{\kappa^2 c^2} - 2\frac{g\sqrt{g}}{\kappa^3 c^3})\bar{T}_{\xi 0} \qquad (92)$$

$$\frac{\partial \bar{p}_1}{\partial \eta} = -\frac{g}{c^2}\frac{1}{\zeta_{s0} - \zeta_b}\frac{1}{\bar{u}_0'}\{(\bar{u}_0'^2 + \bar{v}_0^2)\bar{v}_1 + \bar{u}_0\bar{v}_0\bar{u}_1\} +$$

$$+ \frac{g}{c^2}\frac{\zeta_{s1}}{(\zeta_{s0} - \zeta_b)^2}\bar{u}_0'\bar{v}_0 - (1+3\frac{g}{\kappa^2 c^2} - 2\frac{g\sqrt{g}}{\kappa^3 c^3})\bar{T}_{\eta 0} \qquad (93)$$

This solution will be discussed in chapter VIII.

3. First order approximation of the complete solution.

If an (n)th order approximation $fn(\xi,\eta,\zeta;\varepsilon)$ of the function $f(\xi,\eta,\zeta;\varepsilon)$ is defined by:

$$fn(\xi,\eta,\zeta;\varepsilon) = f(\xi,\eta,\zeta;\varepsilon) + 0(\varepsilon^{n+1}) \tag{94}$$

then the following expressions for u, v and p are first order approximations of the solution of the complete system (28 through 35):

$$u1 = \bar{u}\{1 + \frac{\sqrt{g}}{\kappa C} + \frac{\sqrt{g}}{\kappa C}\ln(1+Z)\} - \varepsilon(\zeta_s - \zeta_b)\,\tilde{u}\,[2F_1(Z) + \frac{\sqrt{g}}{\kappa C}F_2(Z) +$$

$$- 2(1 - \frac{\sqrt{g}}{\kappa C})\{1 + \frac{\sqrt{g}}{\kappa C} + \frac{\sqrt{g}}{\kappa C}\ln(1+Z)\}] \tag{95}$$

$$v1 = \bar{v}\{1 + \frac{\sqrt{g}}{\kappa C} + \frac{\sqrt{g}}{\kappa C}\ln(1+Z)\} - \varepsilon(\zeta_s - \zeta_b)\tilde{v}[2F_1(Z) + \frac{\sqrt{g}}{\kappa C}F_2(Z) +$$

$$- 2(1 - \frac{\sqrt{g}}{\kappa C})\{1 + \frac{\sqrt{g}}{\kappa C} + \frac{\sqrt{g}}{\kappa C}\ln(1+Z)\}] \tag{96}$$

$$p1 = \frac{\zeta_s}{F^2} \tag{97}$$

in which:

$$Z = \frac{\zeta-\zeta_s}{\zeta_s - \zeta_b} \tag{98}$$

$$\tilde{u} = \frac{1}{2\kappa^2\,\bar{u}'^3}\{(\bar{u}'^2 + \bar{v}^2)\,\bar{T}_\xi - \bar{u}\,\bar{v}\,\bar{T}_\eta\} \tag{99}$$

$$\tilde{\bar{v}} = \frac{1}{2\kappa^2 \bar{u}'^3} \{(\bar{u}'^2 + \bar{u}^2)\, \bar{T}_\eta - \bar{u}\, \bar{v}\, \bar{T}_\xi\} \tag{100}$$

$$\bar{T}_\xi = \bar{u} \frac{\partial \bar{u}}{\partial \xi} + v \frac{\partial \bar{u}}{\partial \eta} \tag{101}$$

$$\bar{T}_\eta = \bar{u} \frac{\partial \bar{v}}{\partial \xi} + \bar{v} \frac{\partial \bar{v}}{\partial \eta} \tag{102}$$

$$F_1(Z) = \int_{-1+Z'}^{Z} \frac{\ln(1+Z)}{Z}\, dZ \tag{103}$$

$$F_2(Z) = \int_{-1+Z'}^{Z} \frac{\ln^2(1+Z)}{Z}\, dZ \tag{104}$$

$$Z' = \frac{\zeta'}{\zeta_s - \zeta_b} = \exp(-1 - \frac{\kappa C}{\sqrt{g}}) \tag{105}$$

This solution provides little insight into the physics of the secondary flow. Therefore it will be attempted to express it in a more "physical" way by means of a coordinate-transformation.

Expressions 95 and 96 are hardly influenced by orthogonal transformations of the horizontal coordinates. Only the factors $\tilde{u}$ and $\tilde{v}$ will change. Adopting horizontal coordinates coinciding with the streamlines of the $\bar{u}$, $\bar{v}$-field and their orthogonals, one of the transformed depth-averaged velocity-components, say $\bar{v}$, equals zero by definition. In that case one finds:

$$\tilde{u} = \frac{1}{2\kappa^2} \frac{\bar{T}_s}{\bar{u}} = \frac{1}{2\kappa^2} \frac{\partial \bar{u}}{\partial s} \tag{106}$$

$$\tilde{v} = \frac{1}{\kappa^2} \frac{\bar{T}_n}{\bar{u}} = \frac{1}{\kappa^2} \frac{\bar{u}}{r_s} \tag{107}$$

in which s is the streamwise coordinate and r_s^{-1} is the curvature of the local $\bar{u}$, $\bar{v}$-streamline.
Then the horizontal velocity-components can be written as:

$$u1 = \bar{u}\{1 + \frac{\sqrt{g}}{\kappa C} + \frac{\sqrt{g}}{\kappa C} \ln(1+Z)\} - \varepsilon(\zeta_s - \zeta_b) \frac{1}{2\kappa^2} \frac{\partial \bar{u}}{\partial s} \text{ fsec}(Z) \tag{108}$$

$$v1 = - \varepsilon(\zeta_s - \zeta_b) \frac{1}{\kappa^2} \frac{\bar{u}}{r_s} \text{ fsec}(Z) \tag{109}$$

in which fsec(Z) denotes the normalized vertical distribution of the secondary flow. This has in essence been found by many authors for axisymmetric flow problems. According to 95 and 96 it is given by:

$$\text{fsec}(Z) = 2 F_1(Z) + \frac{\sqrt{g}}{\kappa C} F_2(Z) - 2(1 - \frac{\sqrt{g}}{\kappa C})\{1 + \frac{\sqrt{g}}{\kappa C} + \frac{\sqrt{g}}{\kappa C} * \ln(1+Z)\} \tag{110}$$

A graph of this function is given in fig. 2.
From 108 and 109 it appears that there is a main flow with a vertical distribution like uniform shear flow and a secondary flow due to inertial effects, having a vertical distribution similar to the radial velocity in axisymmetric curved flow (fig. 2). In the present case, however, this secondary flow is in general not perpendicular to the main flow, but has a component in the main flow direction as a result of the longitudinal acceleration of the main flow. As in the case of axisymmetric flow, the transverse component of the secondary flow is caused by centrifugal effects, thus by the curvature of the main flow.

Considering the deviation of the horizontal velocity vector from the direction of the $\bar{u},\bar{v}$-streamlines, eqs. 108 and 109 yield:

$$\tan \phi_v = \frac{vl}{ul} = -\varepsilon(\zeta_s - \zeta_b)\frac{1}{\kappa^2 r_s}\,\mathrm{fdev}(Z) + O(\varepsilon^2) \qquad (111)$$

where: $$\mathrm{fdev}(Z) = \frac{\mathrm{fsec}(Z)}{1 + \frac{\sqrt{g}}{\kappa C} + \frac{\sqrt{g}}{\kappa C}\ln(1+Z)} \qquad (112)$$

Fig.3 gives a graph of this function. Its value at the free surface is:

$$\mathrm{fdev}(0) = \frac{1}{1 + \frac{\sqrt{g}}{\kappa C}}\left\{2\,F_1(0) + \frac{\sqrt{g}}{\kappa C}F_2(0) - 2\left(1 - \frac{g}{\kappa^2 C^2}\right)\right\}$$

$$= \frac{1}{1 + \frac{\sqrt{g}}{\kappa C}}\left\{1.2899 - 2.4041\,\frac{\sqrt{g}}{\kappa C} + 2\,\frac{g}{\kappa^2 C^2}\right\} \qquad (113)$$

Near the bed one finds:

$$\mathrm{fdev}(Z\downarrow -1) = -2\left(1 - \frac{\sqrt{g}}{\kappa C}\right) \qquad (114)$$

The components of the horizontal shear stress follow from the definitions:

$$\tau_{s\zeta} = \alpha_t \frac{\partial u}{\partial \zeta} \qquad \text{and} \qquad \tau_{n\zeta} = \alpha_t \frac{\partial v}{\partial \zeta} \qquad (115)$$

Using expression 42 for α_t and exprs. 108 and 109 for the velocities, the components of 115 can be elaborated to:

$$\tau_{s\zeta} = -\frac{g}{C^2}\bar{u}^2 Z + \varepsilon(\zeta_s - \zeta_b)\,\bar{u}\frac{\partial\bar{u}}{\partial s}\frac{\sqrt{g}}{\kappa C} Z(1+Z)\frac{\partial f_{sec}}{\partial Z} + O(\varepsilon^2) \qquad (116)$$

$$\tau_{n\zeta} = \varepsilon(\zeta_s - \zeta_b)\frac{\bar{u}^2}{r_s}\frac{\sqrt{g}}{\kappa C} Z(1+Z)\frac{\partial f_{sec}}{\partial Z} + O(\varepsilon^2) \qquad (117)$$

The vertical distribution of the "secondary shear stress", $Z(1+Z)\frac{\partial f_{sec}}{\partial Z}$, is given in fig. 4. The values of the bed shear stress components are:

$$\tau_{sbed} \simeq \frac{g}{C^2}\bar{u}^2 + \varepsilon(\zeta_s - \zeta_b)\,\bar{u}\frac{\partial\bar{u}}{\partial s} 2\frac{g}{\kappa^2 C^2}\left(1 - \frac{\sqrt{g}}{\kappa C}\right) \qquad (118)$$

$$\tau_{nbed} \simeq \varepsilon(\zeta_s - \zeta_b)\frac{\bar{u}^2}{r_s} 2\frac{g}{\kappa^2 C^2}\left(1 - \frac{\sqrt{g}}{\kappa C}\right) \qquad (119)$$

So the deviation of the bed shear stress vector from the direction of the $\bar{u},\bar{v}$-streamlines is:

$$\tan\phi_\tau = \frac{2\varepsilon}{\kappa^2}\frac{1}{r_s}\left(1 - \frac{\sqrt{g}}{\kappa C}\right)(\zeta_s - \zeta_b) + \sigma(\varepsilon^2) \qquad (120)$$

Apparently, the directions of the velocity vector at the bed and the bed shear stress vector coincide up to $O(\varepsilon^2)$.

Returning to the Cartesian coordinate-system, the differential equations from which the depth-averaged quantities $\bar{u},\bar{v}$ and $\bar{p}$ must be solved read:

$$\frac{\partial}{\partial \xi}\{\bar{u}(\zeta_s - \zeta_b)\} + \frac{\partial}{\partial \eta}\{\bar{v}(\zeta_s - \zeta_b)\} = 0 \qquad (121)$$

$$\frac{\partial \bar{p}}{\partial \xi} = -\frac{g}{C^2}\frac{\bar{u}\,\bar{u}'}{\zeta_s - \zeta_b} - \varepsilon\left(1 + 3\frac{g}{\kappa^2 C^2} - 2\frac{g\sqrt{g}}{\kappa^3 C^3}\right)\bar{T}_\xi \qquad (122)$$

$$\frac{\partial \bar{p}}{\partial \eta} = -\frac{g}{C^2}\frac{\bar{v}\,\bar{u}'}{\zeta_s - \zeta_b} - \varepsilon\left(1 + 3\frac{g}{\kappa^2 C^2} - 2\frac{g\sqrt{g}}{\kappa^3 C^3}\right)\bar{T}_\eta \qquad (123)$$

The solution of this system will be discussed in chapter VIII. In the equations of motion 122 and 123, there is an extra term in addition to the "uniform flow terms". Apparently, this term arises from inertial effects, but it is not exactly equal to the average of the inertial terms of the main flow, since then the constant should have been

$$1 + \frac{g}{\kappa^2 C^2} \qquad \text{instead of} \qquad 1 + 3\frac{g}{\kappa^2 C^2} - 2\frac{g\sqrt{g}}{\kappa^3 C^3} \qquad (124)$$

as can be shown by averaging u_0^2 over the depth of flow. The rest of the term accounts for the bed shear stress caused by the secondary flow. According to 118 and 119, the secondary bed shear stress is proportional to the inertial terms of the average main flow through the constant

$$2\frac{g}{\kappa^2 C^2}\left(1 - \frac{\sqrt{g}}{\kappa C}\right)$$

which is exactly the difference between the two constants in 124.

Obviously, the secondary bed shear stress is of minor importance in the depth-averaged equations of motion 122 and 123, the factor $g/\kappa^2 C^2$ being small with respect to 1.

4. Solution with rough bed conditions.

In case of a rough bed, at a distance k above the bed the direction of the horizontal shear stress must coincide with the direction of the horizontal velocity. So:

$$\frac{\tau_{\eta\zeta}}{\tau_{\xi\zeta}} = \frac{\frac{\partial v}{\partial \zeta} + \varepsilon^2 \frac{\partial w}{\partial \eta}}{\frac{\partial u}{\partial \zeta} + \varepsilon^2 \frac{\partial w}{\partial \xi}} = \frac{v}{u} \quad \text{at } \zeta = \zeta_b + \frac{k}{d}$$

In the zero order system, this yields:

$$\frac{\frac{\partial v_0}{\partial \zeta}}{\frac{\partial u_0}{\partial \zeta}} = \frac{v_0}{u_0} \quad \text{at } \zeta = \zeta_b + \frac{k}{d}$$

which is automatically satisfied if the vertical distributions of u_0 and v_0 are similar. Hence the system requires another boundary condition in order to be fully determined. Assuming the flow near the bed to be similar to a uniform flow with the same bed shear stress and the same local direction, this condition is:

$$u' = (u^2 + v^2)^{\frac{1}{2}} = \frac{v_*}{\kappa} \left(\frac{\kappa C}{\sqrt{g}} + 1 + \ln \frac{k}{d}\right) \quad \text{at } \zeta = \zeta_b + \frac{k}{d}$$

in which: $v_* = (\tau_{\xi\zeta}^2 + \tau_{\eta\zeta}^2)^{\frac{1}{4}}$

Combining this "velocity-condition" and the abovementioned "shear stress condition", one obtains:

$$\left.\begin{aligned} uu' &= \frac{1}{\kappa^2}\,\alpha_t\,\left(\frac{\partial u}{\partial \zeta} + \varepsilon^2\,\frac{\partial w}{\partial \xi}\right)\left(\frac{\kappa C}{\sqrt{g}} + 1 + \ln\frac{k}{d}\right)^2 \\ vu' &= \frac{1}{\kappa^2}\,\alpha_t\,\left(\frac{\partial v}{\partial \zeta} + \varepsilon^2\,\frac{\partial w}{\partial \eta}\right)\left(\frac{\kappa C}{\sqrt{g}} + 1 + \ln\frac{k}{d}\right)^2 \end{aligned}\right\} \text{ at } \zeta = \zeta_b + \frac{k}{d}$$

Using these boundary conditions, the vertical distributions of the various subfunctions can be solved in the same way as described before.

In axisymmetric flow, the "velocity-conditions" and the "shear stress condition" can be uncoupled, as the main and the secondary flow direction coincide with the tangential and the radial coordinate, respectively. In that case the tangential (main) velocity is solved directly from the equation of motion in tangential direction, using the "velocity-condition" at the bed. Subsequently, the radial (secondary) velocity is solved from the equation of motion in radial direction, using the "shear stress condition" at the bed.

VII. AXISYMMETRIC FLOW

Before going on with the computation of the depth-averaged quantities, the axisymmetric flow problem will receive further attention, in order to compare the present solutions to those of other authors and to experimental results. In fact, the axisymmetric solution is only a special case of the general solution, so it may be obtained by the general procedure described in chapter VIII. Since it allows for a rather simple analytical solution, however, it will be treated separately.

Adopting a cylindrical coordinate system (r,ϕ,ζ) with a vertical axis going through the centre of the circle describing the centreline of the channel, the present solution reads in case of axisymmetric flow:

$$u = \bar{u}\{1 + \frac{\sqrt{g}}{\kappa C} + \frac{\sqrt{g}}{\kappa C}\ln(1+Z)\} \tag{125}$$

$$v = \varepsilon(\zeta_s - \zeta_b)\frac{\bar{u}}{\kappa^2 r}\, f\sec(Z) \tag{126}$$

with the depth-averaged equations:

$$\frac{1}{r}\frac{\partial \bar{p}}{\partial \phi} = -\frac{g}{C^2}\frac{\bar{u}^2}{\zeta_s - \zeta_b} \tag{127}$$

$$\frac{\partial \bar{p}}{\partial r} = \varepsilon\left(1 + 3\frac{g}{\kappa^2 C^2} - 2\frac{g\sqrt{g}}{\kappa^3 C^3}\right)\frac{\bar{u}^2}{r} \tag{128}$$

For geometrical reasons, $\frac{\partial \bar{p}}{\partial \phi}$ must be a constant, say $-\Delta$.

Then:

$$\bar{u} = \frac{C}{\sqrt{g}} \frac{\sqrt{\zeta_s - \zeta_b}}{\sqrt{r}} \sqrt{\Delta} \tag{129}$$

From the integral conservation of mass one can find:

$$\int_{r_i}^{r_o} (\zeta_s - \zeta_b)\, \bar{u}\, dr = \frac{B}{R_0} = r_o - r_i \tag{130}$$

where r_i and r_o are the radius of curvature of the inner and the outer bank, respectively. If $(\zeta_s - \zeta_b)$ is known, Δ can be solved from 129 and 130.

Since $\bar{p} = \zeta_s / F^2$ (eqs. 34 and 58), eq. 128 can be translated into an equation for ζ_s. If, moreover, the origin of the coordinate-system is situated at the average level of the free surface in the ray under consideration, then by definition:

$$\int_{r_i}^{r_o} \zeta_s\, dr = 0 \tag{131}$$

Thus the general solution of ζ_s reads:

$$\zeta_s = K\, e^{-\frac{K}{r}} \{c - \int_{r_i}^{r} e^{\frac{K}{r}} \frac{\zeta_b}{r^2}\, dr\} \tag{132}$$

with: $K = \varepsilon F^2 (1 + 3 \frac{g}{\kappa^2 C^2} - 2 \frac{g\sqrt{g}}{\kappa^3 C^3}) \frac{C^2}{g} \Delta$

$$c = \frac{\int_{r_i}^{r_o} dr\, e^{-\frac{K}{r}} \int_{r_i}^{r} e^{\frac{K}{r}} \frac{\zeta_b}{r^2}\, dr}{\int_{r_i}^{r_o} e^{-\frac{K}{r}}\, dr}$$

Since K (and so Δ) appears in this expression in a rather complex way, it will be hard to solve Δ from 129 and 130. If $\Delta << 1$, however, 132 can be approximated by:

$$\zeta_s = \Delta\, K'\{c_0 - \int_{r_i}^{r} \frac{\zeta_b}{r^2}\, dr\} + 0(\Delta^2) \tag{133}$$

with: $K' = \varepsilon F^2 (1 + 3 \frac{g}{\kappa^2 C^2} - 2 \frac{g\sqrt{g}}{\kappa^3 C^3}) \frac{C^2}{g}$

$$c_0 = \frac{1}{r_0 - r_i} \int_{r_i}^{r_o} dr \int_{r_i}^{r} \frac{\zeta_b}{r^2}\, dr$$

Then $\zeta_s - \zeta_b = -\zeta_b + 0(\Delta)$, whence 129 and 130 yield:

$$\Delta = \frac{g}{C^2} \{ \frac{1}{r_o - r_i} \int_{r_i}^{r_o} (-\zeta_b)^{3/2}\, r^{-1/2}\, dr\}^{-2} + 0(\Delta^2) \tag{134}$$

In case of a flat bed, when $\zeta_b = -1$, this reduces to:

$$\Delta = \frac{g}{C^2} \frac{1}{4} (\sqrt{r_o} + \sqrt{r_i})^2 \tag{135}$$

Hence:

$$\bar{u} = \frac{1}{2} \frac{\sqrt{r_o} + \sqrt{r_i}}{\sqrt{r}} + 0(\Delta) \tag{136}$$

Furthermore:

$$\zeta_s = \Delta K' (\frac{1}{r_o - r_i} \ln \frac{r_o}{r_i} - \frac{1}{r}) + 0(\Delta^2) \tag{137}$$

Hence the superelevation, i.e. the difference in the free surface level between the outer and the inner bank, is given by:

$$\delta\zeta_s = - \Delta K' \left(\frac{1}{r_o} - \frac{1}{r_i}\right) + O(\Delta^2) \qquad (138)$$

This axisymmetric solution can be compared to theoretical and experimental results obtained by other investigators. This will be done separately for the most essential features of the solution.

1. Vertical distribution of the main flow.

Actually, the logarithmic distribution given by 125 is not a result of the analysis but an assumption: this logarithmic profile follows directly from the assumed vertical distribution of the eddy viscosity.
The validity of this assumption was studied extensively by Rozovskii[6], who arrived at the conclusion that the logarithmic law is a good approximation of the main flow profile throughout the bend.
Ever since, the logarithmic law is most widely applied in shallow bend theory. In fig. 1 it is compared to experimental results and to the Boussinesq-Bazin parabola:

$$u = \bar{u} \{1 + \frac{m'}{3} \frac{\sqrt{g}}{C} (1 - 3\zeta^2)\} \text{ with } m' = 6.5 \qquad (139)$$

applied by Engelund[10].

Fig. 1 shows that there is no definite conclusion in favour of either profile as far as the main flow distribution is concerned. The parabola is better in the upper part of the vertical and the logarithm is better in the lower part.

2. Vertical distribution of the radial velocity.

As mentioned before, there are many different opinions about how to compute the radial velocity component. Fig. 2.a gives some of the resulting vertical distributions for a hydraulically smooth bed and some relevant experimental results. Fig. 2.b gives the same for a hydraulically rough bed.
It can be concluded from these figures that eq. 110 provides a fairly good approximation of the measured values, both for smooth and for rough beds.
In addition, figs. 3a and 3b give the vertical distribution of the tangent of the velocity-vector deviation angle for a smooth and a rough bed, respectively. These figures show that the present model (eq. 112) and Engelund's "parabolic model"[10] yield finite deviation tangents when approaching the bed, while Rozovskii's[6] and Ikeda's[11] yield infinite tangents. Since it has been shown experimentally many times that the angle of deviation at the bed is less than 90^{o} (mostly less than 45^{o}), eq. 112 and the parabolic model are preferable in this respect.

3. Vertical distribution of the "secondary shear stress".

The vertical distribution of the "secondary shear stress", i.e. the shear stress component due to the secondary flow, is given in fig. 4.
Fig. 4a (smooth bed) shows that the secondary shear stress tends to vanish near the bed in Rozovskii's and Ikeda's model, but has a finite value in the present (eq. 117) and in Engelund's model.

Fig. 4b (rough bed) shows that Rozovskii's model yields a finite value at the bed now, as well as Engelund's model and eq. 117, but in contrast to Ikeda's.
As the secondary shear stress can not be expected to vanish at the bed in either case, this is another drawback of Ikeda's and Rozovskii's (smooth bed) models.

4. Transverse slope of the free surface .

The expression for the transverse slope of the free surface resulting from the various models always has the form:

$$\frac{\partial \zeta_s}{\partial r} = \varepsilon F^2 \frac{\bar{u}^2}{r} K\left(\frac{C}{\sqrt{g}}\right) \qquad (140)$$

Fig. 5 gives the distribution of K as a function of $C/\sqrt{g}$.
In all models but one (Rozovskii's), K shows a uniformly damping character, with a limit value 1 for large $C/\sqrt{g}$. Only Rozovskii's model yields a distribution of k having a maximum for $C/\sqrt{g} \simeq 9$. The differences between the various models are rather small, however, and there are no experimental data available which are suited to make a distinction between them in this respect. The only information available is provided by B.C. Yen and C.L. Yen[12], whose experiments show that the transverse slope coefficient in a 90° shallow bend with a flat bed is a constant slightly above 1 almost throughout the bend.

Conclusion:

The comparison of the present model with various other models for shallow, axisymmetrical flow shows that the present model yields results which agree fairly well with experiments. Besides, its behaviour is acceptable from a physical point of

view.

Only one of the other models considered shows these features as well, viz. Engelund's parabolic model.

It is rather difficult to decide which of the two models should be preferred, the former being an extension of the logarithmic distribution, which is in accordance with boundary layer theory, the latter being much easier from a computational point of view.

Besides, it turns out that the boundary condition at the bed needs not be different for smooth and rough beds. Both the present (with an essentially smooth bed condition) and Engelund's model (with an essentially rough bed condition) show good agreement with smooth as well as rough bed data.

VIII. COMPUTATION OF THE DEPTH-AVERAGED QUANTITIES

Returning from the axisymmetric problem to the general curved channel problem, the horizontal distribution of the depth-averaged quantities is still to be determined. This could be done in two different ways:

- following the successive approximations of chapter VI, i.e. solve the zero order depth-averaged system 67-69, subsequently the first order system 91-93 (the zero order quantities in it being known functions then), etc. Finally, the subfunctions can be composed to a certain approximation of the complete solution.
- solving the first order approximation of the complete depth-averaged system 121-123 directly.

Both approaches will be discussed in this chapter, but the first one only as far as the zero order system is involved, as all higher order systems allow for the same computational procedure.

1. Solution of the zero order depth-averaged system.

According to chapter VI, the depth-averaged quantities $\bar{u}_0$, $\bar{v}_0$ and $\bar{p}_0$ must be solved from:

$$\frac{1}{\zeta_{s0} - \zeta_b}\left[\frac{\partial}{\partial \xi}\{\bar{u}_0(\zeta_{s0} - \zeta_b)\} + \frac{\partial}{\partial \eta}\{\bar{v}_0(\zeta_{s0} - \zeta_b)\}\right] \qquad (67)$$

$$\frac{\partial \bar{p}_0}{\partial \xi} = - \frac{g}{c^2} \frac{\bar{u}_0 \bar{u}_0'}{\zeta_{s0} - \zeta_b} \qquad (68)$$

$$\frac{\partial \bar{p}_0}{\partial \eta} = - \frac{g}{c^2} \frac{\bar{v}_0 \bar{u}_0'}{\zeta_{s0} - \zeta_b} \qquad (69)$$

Eliminating $\bar{p}_0$ from the latter two equations, one finds after some elaboration:

$$2\,\bar{u}_0'\,\omega_0 - \frac{\bar{u}_0'^2}{r_{s0}} - \frac{\bar{u}_0'}{\zeta_{s0} - \zeta_b}\left(\bar{u}_0\frac{\partial\zeta_b}{\partial\eta} - \bar{v}_0\frac{\partial\zeta_b}{\partial\xi}\right) = 0 \qquad (141)$$

in which r_{s0} is the radius of curvature of the streamlines of the $\bar{u}_0$, $\bar{v}_0$- field as derived in appendix IV, while the vorticity ω_0 is defined by:

$$\omega_0 = \frac{\partial\bar{v}_0}{\partial\xi} - \frac{\partial\bar{u}_0}{\partial\eta} \qquad (142)$$

Defining the streamfunction Φ_0 by:

$$\bar{u}_0 = \frac{1}{\zeta_{s0} - \zeta_b}\frac{\partial\Phi_0}{\partial\eta} \quad \text{and} \quad \bar{v}_0 = \frac{-1}{\zeta_{s0} - \zeta_b}\frac{\partial\Phi_0}{\partial\xi} \qquad (143)$$

the equation of continuity 67 is satisfied. Substituting 143 into 142 finally yields the relation between stream function and vorticity:

$$\nabla^2\Phi_0 = -(\zeta_{s0} - \zeta_b)\omega_0 + \bar{u}_0\frac{\partial\zeta_b}{\partial\eta} - \bar{v}_0\frac{\partial\zeta_b}{\partial\xi} \qquad (144)$$

in which $\nabla^2\Phi_0 = \frac{\partial^2\Phi_0}{\partial\xi^2} + \frac{\partial^2\Phi_0}{\partial\eta^2}$.

Using 141, one obtains from this relation:

$$\nabla^2\Phi_0 = -\frac{1}{2}(\zeta_{s0} - \zeta_b)\frac{\bar{u}_0'}{r_{s0}} + \frac{3}{2}\left(\bar{u}_0\frac{\partial\zeta_b}{\partial\eta} - \bar{v}_0\frac{\partial\zeta_b}{\partial\xi}\right) \qquad (145)$$

The elevation of the free surface ζ_{s0} can be solved from:

$$\frac{\partial \zeta_{s0}}{\partial \xi} = - F^2 \frac{g}{C^2} \frac{\bar{u}_0 \bar{u}_0'}{\zeta_{s0} - \zeta_b} \tag{146}$$

$$\frac{\partial \zeta_{s0}}{\partial \eta} = - F^2 \frac{g}{C^2} \frac{\bar{v}_0 \bar{u}_0'}{\zeta_{s0} - \zeta_b} \tag{147}$$

which can be transformed to the Poisson equation:

$$\nabla^2 \zeta_{s0} = - F^2 \frac{g}{C^2} \frac{1}{(\zeta_{s0} - \zeta_b)} \frac{\bar{u}_0'^2}{r_{n0}} - 3 F^2 \frac{g}{C^2} \frac{\bar{u}_0'}{(\zeta_{s0} - \zeta_b)^2} * \left(\bar{u}_0 \frac{\partial \zeta_b}{\partial \xi} + \bar{v}_0 \frac{\partial \zeta_b}{\partial \eta}\right) - 3 F^4 \frac{g^2}{C^4} \frac{\bar{u}_0'^3}{(\zeta_{s0} - \zeta_b)^3} \tag{148}$$

in which r_{n0} is the radius of curvature of the curves normal to the streamlines of the $\bar{u}_0$, $\bar{v}_0$-field as derived in appendix IV.

The system to be solved consists of eqs 143, 145 and 148. The relevant boundary conditions are provided by the zero normal velocity- component at the banks and by the inflow and outflow conditions (e.g. a prescribed velocity-distribution at the inflow boundary and a prescribed free surface elevation at the outflow boundary). The following iterative procedure could be adopted for solving this system:

1. Make a first estimate of the velocity field by taking, for instance, the potential flow distribution, following from:

$$\nabla^2 \Phi_0 = 0 \tag{150}$$

2. Determine the radii of curvature r_{s0} and r_{n0} from this velocity-field, using the expressions given in appendix IV.
3. Determine the boundary conditions for the free surface elevation by integration along the banks of:

$$\frac{\partial \zeta_{s0}}{\partial s} = - F^2 \frac{g}{C^2} \frac{\bar{u}_0'^2}{\zeta_{s0} - \zeta_b} \tag{151}$$

   in which s denotes a coordinate along the bank. The value of ζ_{s0} in the right hand part of this equation must be estimated.
4. Solve ζ_{s0} from eq. 148.
5. Solve a new Φ_0 from eq. 145.
6. Determine the new velocity-field.
7. Repeat the procedure from 2. on until the quantities have reached their final value (i.e. until some termination criterion is satisfied).

As an example, the zero order solution of a simple curved flow problem has been determined using a similar iterative procedure. The problem concerns a 180^o curved flume with straight tangent sections at either end of the bend and a rectangular cross-section, having the dimensions:

$R_0 = 4.25$ m ; B = 1.70 m ; $\underline{d} = 0.18$ m ; L = 6.00 m

L being the length of the tangent sections. The flow parameters are:

$V^2/g\underline{d} = 0.215$; $C^2/g = 330$; $\kappa = 0.4$

The bed is flat and horizontal ($\zeta_b = -1.00$) and the inflow and outflow conditions are:

- a constant velocity along the upstream boundary: $\bar{u}'_0 = 1.00$
- a vanishing free surface elevation at the downstream end: $\zeta_{s0} = 0$.

Fig. 6 gives some results of this computation, viz. the distribution of the total velocity $\bar{u}'_0$ and the free surface elevation ζ_{s0}.

Apparently, the zero order system gives neither an adequate description of the depth-averaged velocity-field nor of the free surface elevation.

The most striking phenomena observed in experiments as well as in natural rivers are poorly represented: the transverse slope of the free surface and the shift of the velocity-maximum from the inner to the outer bank.

This is to be expected, however, since the zero order system only concerns the continuity and the bed shear stress of the main flow, but no inertia effects at all; the typical inertia effects mentioned above are not included in the system. Actually, the zero order solution is the curved uniform flow mentioned before.

In order to improve the model, the first order system 91-93 must be solved in addition. Although the first order equations look more complex than the zero order ones, the solution procedure is identical, since all additional terms consist of known zero order quantities. Therefore it will not be described here. The execution of the computation requires rather extensive calculations as a consequence of the complex additional terms. Besides, it will be shown that the solution of the first order approximation of the complete system is preferable from a mathematical point of view.

Therefore the first order system will not be solved separately for the present example.

2. First order approximation of the complete solution.

As follows from chapter IV, the first order accurate depth-averaged quantities $\bar{u}$, $\bar{v}$ and $\bar{p}$ must be solved from:

$$\frac{\partial}{\partial \xi}\{\bar{u}(\zeta_s - \zeta_b)\} + \frac{\partial}{\partial \eta}\{\bar{v}(\zeta_s - \zeta_b)\} = 0 \qquad (121)$$

$$\frac{\partial \bar{p}}{\partial \xi} = -\frac{g}{C^2}\frac{\bar{u}'\bar{u}}{\zeta_s - \zeta_b} - \varepsilon\left(1 + 3\frac{g}{\kappa^2 C^2} - 2\frac{g\sqrt{g}}{\kappa^3 C^3}\right)\bar{T}_\xi \qquad (122)$$

$$\frac{\partial \bar{p}}{\partial \eta} = -\frac{g}{C^2}\frac{\bar{u}'\bar{v}}{\zeta_s - \zeta_b} - \varepsilon\left(1 + 3\frac{g}{\kappa^2 C^2} - 2\frac{g\sqrt{g}}{\kappa^3 C^3}\right)\bar{T}_\eta \qquad (123)$$

Eliminating $\bar{p}$ from the latter two equations and elaborating the result, accounting for the equation of continuity 121 and for $\zeta_s = F^2\bar{p}$, the following equation is found:

$$-\frac{g}{C^2}\frac{1}{\zeta_s - \zeta_b}\{2\bar{u}'\omega - \frac{\bar{u}'^2}{r_s} + \frac{\bar{u}'}{\zeta_s - \zeta_b}\left(\bar{v}\frac{\partial \zeta_b}{\partial \xi} - \bar{u}\frac{\partial \zeta_b}{\partial \eta}\right) -$$

$$-\varepsilon F^2 K \frac{1}{\zeta_s - \zeta_b}\frac{\bar{u}'^4}{r_s}\} - \varepsilon K\{\frac{\partial}{\partial \xi}(\bar{u}\omega) + \frac{\partial}{\partial \eta}(\bar{v}\omega)\} = 0 \qquad (152)$$

in which $K = 1 + 3\frac{g}{\kappa^2 C^2} - 2\frac{g\sqrt{g}}{\kappa^3 C^3}$

r_s = radius of curvature of the streamlines of the $\bar{u},\bar{v}$-field as derived in appendix IV

$\omega = \frac{\partial \bar{v}}{\partial \xi} - \frac{\partial \bar{u}}{\partial \eta}$ = the vorticity of the depth-averaged flow.

Eq. 152 can be elaborated to:

$$\frac{\partial}{\partial\xi}(\bar{u}\omega) + \frac{\partial}{\partial\eta}(\bar{v}\omega) = -\frac{g}{\varepsilon C^2}\frac{1}{K}\frac{\bar{u}'}{\zeta_s - \zeta_b}2\omega + \frac{g}{\varepsilon C^2}\frac{1}{K}\frac{\bar{u}'}{\zeta_s - \zeta_b} *$$

$$\left(1 + \varepsilon F^2 \frac{\bar{u}'^2}{\zeta_s - \zeta_b}\right)\frac{\bar{u}'}{r_s} +$$

$$-\frac{g}{\varepsilon C^2}\frac{1}{K}\frac{\bar{u}'^2}{(\zeta_s - \zeta_b)^2}\left(\bar{v}\frac{\partial\zeta_b}{\partial\xi} - \bar{u}\frac{\partial\zeta_b}{\partial\eta}\right) \qquad (153)$$

The equation of continuity is satisfied by defining a stream function Φ such that:

$$\bar{u} = \frac{1}{\zeta_s - \zeta_b}\frac{\partial\Phi}{\partial\eta} \quad \text{and} \quad \bar{v} = \frac{-1}{\zeta_s - \zeta_b}\frac{\partial\Phi}{\partial\xi} \qquad (154)$$

Substituting this into the definition of ω, the following relation between the stream function and the vorticity is obtained:

$$\nabla^2\Phi = -(\zeta_s - \zeta_b)\omega + \left(\bar{v}\frac{\partial\zeta_b}{\partial\xi} - \bar{u}\frac{\partial\zeta_b}{\partial\eta}\right) - \varepsilon F^2 K\frac{\bar{u}'^3}{r_s} \qquad (155)$$

in which: $\nabla^2\Phi = \frac{\partial^2\Phi}{\partial\xi^2} + \frac{\partial^2\Phi}{\partial\eta^2}$

The first order approximation of the free surface elevation ζ_s can be solved from:

$$\frac{\partial \zeta_s}{\partial \xi} = - F^2 \frac{g}{C^2} \frac{\bar{u}'\bar{u}}{\zeta_s - \zeta_b} - \varepsilon F^2 K \bar{T}_\xi \qquad (156)$$

$$\frac{\partial \zeta_s}{\partial \eta} = - F^2 \frac{g}{C^2} \frac{\bar{u}'\bar{v}}{\zeta_s - \zeta_b} - \varepsilon F^2 K \bar{T}_\eta \qquad (157)$$

These equations can be transformed to a Poisson equation in the same way as it was done for the zero order system:

$$\nabla^2 \zeta_s = q(\xi,\eta) \qquad (158)$$

in which $q(\xi,\eta)$ is a fairly extensive expression containing $\bar{u}'$, r_n, $\bar{T}_\xi$ and $\bar{T}_\eta$.

The system of equations to be solved consists of eqs. 153, 154, 155 and 158 and the solution procedure is chosen similar to the procedure applied to the zero order system, but here the computation of the vorticity from the transport equation 153 must be added.

Before doing so, however, it is worthwile to pay some further attention to the vorticity transport equation 153. This equation can be written as a conservation law, reading:

$$\frac{1}{\zeta_s - \zeta_b} \left[\frac{\partial}{\partial \xi} \{\bar{u}(\zeta_s - \zeta_b)\omega\} + \frac{\partial}{\partial \eta} \{\bar{v}(\zeta_s - \zeta_b)\omega\}\right] =$$

$$\frac{\omega}{\zeta_s - \zeta_b}\left[\bar{u} \frac{\partial}{\partial \xi} (\zeta_s - \zeta_b) + \bar{v} \frac{\partial}{\partial \eta} (\zeta_s - \zeta_b)\right] + \text{the right hand}$$

side of eq. 153 (159)

The left hand side of this equation is equivalent to

$$\bar{u}' \frac{\partial \omega}{\partial s}$$

s denoting a (curvilinear) coordinate along the streamlines of the $\bar{u}$, $\bar{v}$-field. Besides

$$\bar{u} \frac{\partial \zeta_s}{\partial \xi} + \bar{v} \frac{\partial \zeta_s}{\partial \eta} = - F^2 \frac{g}{C^2} \frac{\bar{u}'^3}{\zeta_s - \zeta_b} - \varepsilon F^2 K \left(\bar{u} \bar{T}_\xi + \bar{v} \bar{T}_\eta \right) \qquad (160)$$

$$\bar{u} \frac{\partial \zeta_b}{\partial \xi} + \bar{v} \frac{\partial \zeta_b}{\partial \eta} = \frac{1}{\zeta_s - \zeta_b} \left(\frac{\partial \Phi}{\partial \eta} \frac{\partial \zeta_b}{\partial \xi} - \frac{\partial \Phi}{\partial \xi} \frac{\partial \zeta_b}{\partial \eta} \right)$$

$$= \frac{-1}{\zeta_s - \zeta_b} (\mathrm{grad}\Phi \times \mathrm{grad}\, \zeta_b) = \bar{u}' \frac{\partial \zeta_b}{\partial s} \qquad (161)$$

$$\bar{v} \frac{\partial \zeta_b}{\partial \xi} - \bar{u} \frac{\partial \zeta_b}{\partial \eta} = \frac{-1}{\zeta_s - \zeta_b} \left(\frac{\partial \Phi}{\partial \xi} \frac{\partial \zeta_b}{\partial \xi} + \frac{\partial \Phi}{\partial \eta} \frac{\partial \zeta_b}{\partial \eta} \right)$$

$$= \frac{-1}{\zeta_s - \zeta_b} (\mathrm{grad}\Phi . \mathrm{grad}\, \zeta_b) = - \bar{u}' \frac{\partial \zeta_b}{\partial n} \qquad (162)$$

n being a coordinate along the curves normal to the streamlines of the $\bar{u}$, $\bar{v}$-field. The n, s-coordinate-system will be referred to as the streamline-coordinate system.
After some elaboration and division by $\bar{u}'$, eq. 159 yields:

$$\frac{\partial \omega}{\partial s} + f_1(s,n) = f_2(s,n) \qquad (163)$$

with: $$f_1(s,n) = \frac{2}{\zeta_s - \zeta_b} \frac{g}{\varepsilon C^2} \frac{1}{K} + \frac{1}{1 - \varepsilon F^2 K \frac{\bar{u}'^2}{\zeta_s - \zeta_b}} \left\{ \frac{1}{\zeta_s - \zeta_b} \frac{\partial \zeta_b}{\partial s} + \right.$$

$$\left. + F^2 \frac{g}{C^2} \frac{\bar{u}'^2}{(\zeta_s - \zeta_b)^2} + \varepsilon F^2 K \frac{\bar{u}'}{\zeta_s - \zeta_b} \frac{\bar{u}'}{r_n} \right\}$$

$$f_2(s,n) = \{\frac{1}{\zeta_s - \zeta_b} \frac{g}{\varepsilon C^2} \frac{1}{K} + F^2 \frac{g}{C^2} \frac{\bar{u}'^2}{(\zeta_s - \zeta_b)^2}\} \frac{\bar{u}'}{r_s} +$$

$$+ \frac{\bar{u}'}{(\zeta_s - \zeta_b)^2} \frac{g}{\varepsilon C^2} \frac{1}{K} \frac{\partial \zeta_b}{\partial n}$$

So, if the velocity field and the free surface elevation are known, f_1 and f_2 are known functions independent on ω. Then ω reads:

$$\omega = \exp(-\int_0^s f_1 ds)\left[\int_0^s f_2 \exp(+\int_0^s f_1 ds)\, ds + \text{constant}\right] \qquad (164)$$

where the constant is determined by a boundary condition. Apparently, ω has to be prescribed in one point of everey streamline in order to make the solution fully determined. Thus, if no streamline separation occurs at the banks, it is sufficient to prescribe ω in one ray (which intersects all streamlines).
Considering the equations for the free surface elevation 156 and 157 from the same point of view, they can be written as:

$$\frac{\partial \zeta_s}{\partial s} = - F^2 \frac{g}{C^2} \frac{\bar{u}'^2}{\zeta_s - \zeta_b} - \varepsilon F^2 K \bar{u}' \frac{\partial \bar{u}'}{\partial s} \qquad (165)$$

$$\frac{\partial \zeta_s}{\partial n} = - \varepsilon F^2 K \frac{\bar{u}'^2}{r_s} \qquad (166)$$

The latter equation is equivalent to the well-known axisymmetric transverse surface slope equation.
Rewriting eq. 165 as:

$$\frac{\partial}{\partial s}\left(\zeta_s + \varepsilon F^2 K \frac{\bar{u}'^2}{2}\right) = - F^2 \frac{g}{C^2} \frac{\bar{u}'^2}{\zeta_s - \zeta_b} \qquad (167)$$

it is equivalent to the well-known energy equation holding along a streamline.

Writing the solution of this equation in its integral form:

$$\zeta_s = - \varepsilon F^2 K \frac{\bar{u}'^2}{2} - F^2 \frac{g}{C^2} \int_0^s \frac{\bar{u}'^2}{\zeta_s - \zeta_b} ds + \text{constant} \qquad (168)$$

shows that ζ_s must be prescribed also in only one ray to make the solution fully determined.

Making use of these results, one can develop a variant to the computational procedure used to solve the zero order system. It is an iterative procedure involving the following steps:

1. Make a first estimate of the velocity-field, for instance by taking the potential flow distribution.
2. Determine by interpolation the streamlines of this velocity-field, being contourlines of the stream function surface.
3. Determine the radii of curvature of the streamlines and their normals, r_s and r_n, respectively.
4. Compute the free surface elevation by applying 168 along the streamlines.
5. Compute the vorticity by applying 164 along the streamlines.
6. Solve a new Φ from eq. 155.
7. Determine the new velocity-field using 154.
8. Repeat the procedure form 2 on, until a termination criterion is satisfied.

The disadvantage of this procedure is the great number of interpolations, since the Poisson-equation 155 is solved in a coordinate-system which differs from the streamlines. This introduces an extra source of inaccuracy. On the other hand, it is possible to apply the method to more complex geometries, since the Poisson-equation can be solved using a finite element method and the method of computation of the vorticity and the free surface elevation is not influenced by the geometry. Thus the problems at the boundaries arising in finite difference methods are avoided.

The only complication is the determination of r_s and r_n, since the expressions derived in appendix IV can no longer be used. This may not be an obstacle, since there are other methods to determine the curvature of a given curve.

Using the procedure described here, one can find the first order approximation of the complete solution. This has been done for the previous example, yielding the results represented in fig. 6. It turns out that, in contrast with the zero order solution, the velocity-maximum tends to move outward, but much less than observed in experiments. This discrepancy will further be analysed in chapter X.
Besides, fig. 6b shows that the first order approximation yields a somewhat larger average free surface slope than the zero order system. Neither approximation agrees well with the measured data, however, even though in the first order approximation a transverse surface slope occurs. The computed superelevation is larger than the measured one and the computed transverse configuration in the curved section should be "lifted" in order to cope with the experimental data. These discrepancies can be explained from the differences between the measured and the computed velocity-distributions.

IX. ACCURACY OF THE APPROXIMATIONS

The foregoing chapter shows that the paratmeters influencing the solution are:

- the length-scale ratio ε,
- the Froudenumber εF^2,
- the friction factor $\sqrt{g}/\kappa C$.

Since the latter parameter may become rather small (say $.2>\sqrt{g}/\kappa C>.1$), special attention must be paid to the validity (accuracy) of the various approximations of the complete solution.

1. Zero order approximation.

Neglecting the first order terms in the first order approximation of the complete solution represented by eqs. 95-105 and 121-123, the zero order approximation is found to be:

$$u = \bar{u}\,\{1 + \frac{\sqrt{g}}{\kappa C} + \frac{\sqrt{g}}{\kappa C}\ln(1+Z)\} + 0\,\{\varepsilon(\frac{\sqrt{g}}{\kappa C})^0\} \tag{169}$$

$$v = \bar{v}\,\{1 + \frac{\sqrt{g}}{\kappa C} + \frac{\sqrt{g}}{\kappa C}\ln(1+Z)\} + 0\,\{\varepsilon(\frac{\sqrt{g}}{\kappa C})^0\} \tag{170}$$

with $$\frac{\partial}{\partial\xi}\{\bar{u}(\zeta_s - \zeta_b)\} + \frac{\partial}{\partial\eta}\{\bar{v}(\zeta_s - \zeta_b)\} = 0 + 0\,\{\varepsilon(\frac{\sqrt{g}}{\kappa C})^0\} \tag{171}$$

$$\frac{\partial\bar{p}}{\partial\xi} = -\frac{g}{C^2}\frac{\bar{u}'\bar{u}}{\zeta_s - \zeta_b} + 0\{\varepsilon(\frac{\sqrt{g}}{\kappa C})^0\} \tag{172}$$

$$\frac{\partial\bar{p}}{\partial\eta} = -\frac{g}{C^2}\frac{\bar{u}'\bar{v}}{\zeta_s - \zeta_b} + 0\{\varepsilon(\frac{\sqrt{g}}{\kappa C})^0\} \tag{173}$$

This zero order approximation is reliable only if the error in the latter equations is much smaller than the other terms. Consequently:

$$\varepsilon << \frac{g}{C^2} \tag{174}$$

Actually, this is a direct consequence of setting Re' = 1 in the normalization of the system (i.e. supposing the friction to be dominant).

Doing so, it is assumed that the terms

$$\frac{\partial}{\partial\zeta}(\alpha\frac{\partial u}{\partial\zeta}) \qquad \text{and} \qquad \frac{\partial}{\partial\zeta}(\alpha\frac{\partial v}{\partial\zeta})$$

in the normalized system are of the order of magnitude 0(1). If $\bar{u}'$, $\bar{u}$, $\bar{v}$ and $\zeta_s - \zeta_b$ all are of the order 0(1), this implies:

$$\frac{g}{C^2} = 0(\varepsilon^0)$$

which is equivalent to 174.

2. First order approximation.

There are many ways to generate a first order approximation of the complete solution, but only two possibilities will be considered here:

a. the sum of the solution of the zero order system and ε times the solution of the first order system,
b. the first order approximation described by eqs. 95-105 and 121-123.

In order to obtain an impression about the accuracy of these approximate solutions, the second order system must be considered. Giving only the terms that are of interest here, the solution of this system reads:

$$u_2 = \left[\bar{u}\{1 + \frac{\sqrt{g}}{\kappa C} + \frac{\sqrt{g}}{\kappa C}\ln(1+Z)\}\right]_2 - \left[(\zeta_s - \zeta_b)\,\bar{u}\,\text{fsec}(Z)\right]_1 + \text{other terms } 0(\frac{\kappa C}{\sqrt{g}}) \qquad (175)$$

in which the subscripts of the expressions between brackets in-

dicate which subfunction of the relevant expression is concerned. A similar expression is found for v_2.
The depth-averaged second order equations read:

$$\frac{\partial}{\partial\xi}\left[\bar{u}(\zeta_s-\zeta_b)\right]_2 + \frac{\partial}{\partial\eta}\left[\bar{v}(\zeta_s-\zeta_b)\right]_2 = 0 \tag{176}$$

$$\frac{\partial\bar{p}_2}{\partial\xi} = -\left[\frac{g}{C^2}\frac{\bar{u}'\bar{u}}{\zeta_s-\zeta_b}\right]_2 - K\left[\bar{T}_\xi\right]_1 + \text{other terms } O(\frac{\sqrt{g}}{\kappa C}) \tag{177}$$

$$\frac{\partial\bar{p}_2}{\partial\eta} = -\left[\frac{g}{C^2}\frac{\bar{u}'\bar{v}}{\zeta_s-\zeta_b}\right]_2 - K\left[\bar{T}_\eta\right]_1 + \text{other terms } O(\frac{\sqrt{g}}{\kappa C}) \tag{178}$$

Consequently the second order approximation of the complete solution can be written as:

$$u = \bar{u}\{1 + \frac{\sqrt{g}}{\kappa C} + \frac{\sqrt{g}}{\kappa C}\ln(1+Z)\} - \varepsilon(\zeta_s-\zeta_b)\,\tilde{u}\,\text{fsec}(Z) + \text{terms } O(\varepsilon\frac{2\kappa C}{\sqrt{g}})$$

$$v = \bar{v}\{1 + \frac{\sqrt{g}}{\kappa C} + \frac{\sqrt{g}}{\kappa C}\ln(1+Z)\} - \varepsilon(\zeta_s-\zeta_b)\,\tilde{v}\,\text{fsec}(Z) + \text{terms } O(\varepsilon\frac{2\kappa C}{\sqrt{g}})$$

with the depth-averaged equations:

$$\frac{\partial}{\partial\xi}\{\bar{u}\,(\zeta_s-\zeta_b)\} + \frac{\partial}{\partial\eta}\{\bar{v}\,(\zeta_s-\zeta_b)\} = 0 \tag{181}$$

$$\frac{\partial\bar{p}}{\partial\xi} = -\frac{g}{C^2}\frac{\bar{u}'\bar{u}}{\zeta_s-\zeta_b} - \varepsilon K\,\bar{T}_\xi + \text{terms } O(\varepsilon^2\frac{\sqrt{g}}{\kappa C}) \tag{182}$$

$$\frac{\partial\bar{p}}{\partial\eta} = -\frac{g}{C^2}\frac{\bar{u}'\bar{v}}{\zeta_s-\zeta_b} - \varepsilon K\,\bar{T}_\xi + \text{terms } O(\varepsilon^2\frac{\sqrt{g}}{\kappa C}) \tag{183}$$

a. Accuracy of the weighted sum approximation.

Adopting the weighted sum of the solutions of the zero and first order systems as the first order approximation of the complete solution, none of the second order terms is taken into account. Consequently, this approximation can be written as:

$$u = \left[\bar{u}\left\{1 + \frac{\sqrt{g}}{\kappa C} + \frac{\sqrt{g}}{\kappa C}\ln(1+Z)\right\}\right]_{0 + \varepsilon*1} - \varepsilon\left[(\zeta_s - \zeta_b)\,\tilde{u}\,\mathrm{fsec}(Z)\right]_0 + \\ + 0\left(\varepsilon^2\frac{\kappa C}{\sqrt{g}}\right) \qquad (184)$$

where the subscripts of the expressions between brackets indicate which combination of subfunctions of the relevant expression is concerned.

For v a similar expression is found.

The relevant depth-averaged equations read:

$$\left[\frac{\partial}{\partial\xi}\{\bar{u}(\zeta_s-\zeta_b)\}\right]_{0 + \varepsilon*1} + \left[\frac{\partial}{\partial\eta}\{\bar{v}(\zeta_s-\zeta_b)\}\right]_{0 + \varepsilon*1} = 0 + 0(\varepsilon^2) \qquad (185)$$

$$\left[\frac{\partial\bar{p}}{\partial\xi}\right]_{0 + \varepsilon*1} = -\frac{g}{C^2}\left[\frac{\bar{u'}\bar{u}}{\zeta_s-\zeta_b}\right]_{0 + \varepsilon*1} - \varepsilon K\left[\bar{T}_\xi\right]_0 + 0(\varepsilon^2) \qquad (186)$$

$$\left[\frac{\partial\bar{p}}{\partial\eta}\right]_{0 + \varepsilon*1} = -\frac{g}{C^2}\left[\frac{\bar{u'}\bar{v}}{\zeta_s-\zeta_b}\right]_{0 + \varepsilon*1} - \varepsilon K\left[\bar{T}_\eta\right]_0 + 0(\varepsilon^2) \qquad (187)$$

Requiring the error in each expression to be much smaller than each of the other terms in that expression, one finds as limitations of ε:

- in the expressions for u and v: $\varepsilon \ll \sqrt{g}/\kappa C$ (188)
- in the depth-averaged equations: $\varepsilon \ll \sqrt{g}/\kappa C$ (189)

b. Accuracy of the solution of the first order equation system.
The solution of the first order approximation of the complete system, given by eqs. 95-105, can be written:

$$u = \bar{u}\{1 + \frac{\sqrt{g}}{\kappa C} + \frac{\sqrt{g}}{\kappa C}\ln(1+Z)\} - \varepsilon(\zeta_s-\zeta_b)\,\tilde{u}\,f\sec(Z) + O(\varepsilon^2\frac{\kappa C}{\sqrt{g}}) \qquad (190)$$

and a similar expression for v. The depth-averaged equations are identical to eqs. 181-183.
Hence the following limitations of ε are found:
- in the expression for u and v: $\varepsilon << \sqrt{g}/\kappa C$ (191)
- in the depth-averaged equations: $\varepsilon^2 << \sqrt{g}/\kappa C$ (192)

As shown by 187 and 192, the difference between the two first order approximations is formed by the accuracy of the depth-averaged equations: the solution of the first order equation system yields results which are a factor $\sqrt{g}/\kappa C$ more accurate than the weighted sum approximation.

X. COMPARISON WITH EXPERIMENTS

In order to find out to what extent the model is able to predict an actual flow field, several experiments have been simulated, covering the most important features included in the model.

A. Flat bed experiments.

1. LFM-experiments.

In the Laboratory of Fluid Mechanics of the Dept. of Civil Engineering, Delft University of Technology, a 180^{o} curved flume of the following dimensions has been constructed:

$$R_0 = 4.25 \text{ m} \quad ; \quad B = 1.70 \text{ m} \quad ; \quad L = 6.00 \text{ m}$$

L being the length of the straight tangent reaches upstream and downstream of the curved section. In this flume flat bed experiments have been conducted, i.a. with the following data:

$$\underline{d} = 0.18 \text{ m} \quad ; \; V^2/g\underline{d} = 0.215 \quad ; \quad C^2/g = 330 \text{ (smooth bed)}$$

$$\underline{d} = 0.175 \text{ m} \; ; \; V^2/g\underline{d} = 0.215 \quad ; \quad C^2/g = 97 \quad \text{(rough bed)}$$

In both experiments the inflow conditions were:
- a constant velocity along the upstream boundary
- a vanishing free surface elevation at the downstream weir.

Besides, in the numerical simulation the vorticity was assumed to vanish at the upstream boundary, which was acceptable in view of the long straight reach before the bend.
The measured and computed values of the total velocity and the free surface elevation for the smooth bed case are represented in fig. 6, together with the results of the zero order computation described in chapter VIII.
As can be seen from fig 6.a, the velocity-distribution is re-

presented quite well in the first part of the flume (say up to 30^{o} in the bend), but further on the experimental data show a gradual shift of the velocity-maximum from the inner to the outer wall, which is very poorly represented by the computed data, even though the first order approximation shows a slight shift in the downstream tangent. In the rough bed computations represented in fig. 7, the shift is somewhat stronger, but not sufficient to approximate the measured velocities satisfactorily.
The computed free surface elevation (fig 6.b) does not agree with the experiments either, as was stated already in chapter VIII. There is good agreement as far as the fall over the entire flume is concerned, but this is no merit of the model, but rather an imposed feature, since Chezy's constant is chosen such that this fall is obtained. Using this value of C in the zero order computation, however, the fall turns out be somewhat smaller (about 12%). This phenomenon could be explained from the zero order equation of motion along a streamline 151 and its first order counterpart, eq. 165. The only difference arises from the term:

$$- \varepsilon F^2 K \, \bar{u}' \, \frac{\partial \bar{u}'}{\partial s}$$

accounting for the inertial effects of the main flow and the streamwise component of the shear stress caused by the secondary flow. Both effects work out in the same way, causing the extra head loss computed in the first order approximation.

2. Rozovskii's experiment no. 1.

The LFM-flume mainly consists of plastered masonry, but the outer wall of the curved section is formed by much smoother glass-panels. In order to eliminate this as a possible source of discrepancies between measured and computed data, another smooth bed experiment in a flume with uniform wall roughness was simulated numerically, viz. Rozovskii's exp. no. 1 with the flume

geometry:

$$R_0 = 0.80 \text{ m} \quad ; \quad b = 0.80 \text{ m} \quad ; \quad L = 3.00 \text{ m}$$

and the flow conditions:

$$\underline{d} = 0.06 \text{ m} \; ; \; V^2/g\underline{d} = 0.114 \quad ; \quad C^2/g = 366$$

The inflow and outflow conditions were the same as in the simulation of the LFM-experiments.
Fig. 8a gives the total mean velocity-distribution found from this experiment and the numerical simulation. It shows the same kind of discrepancies as fig. 6a, but more intensively as a consequence of the greater curvature.
This suggests the bank roughness has no important influence on the distribution of the depth-averaged velocities at some distance from the banks.
The water surface configuration (fig. 8b) is predicted fairly well as far as the superelevation is concerned, but the computed head loss is smaller than the measured one.

3. B.C. Yen's experiment.
Anticipating the simulation of C.L. Yen's [13] "equilibrium bed experiments", the flat bed experiments in the same flume reported by B.C. Yen[14] were simulated. The flume consisted of two opposite 90^o curved sections with a 4.27 m (14 ft) straight reach between them and 2.13 m (7 ft) tangent reaches at the upstream and downstream end. In B.C. Yen's experiment the channel had a trapezoidal cross-section with the banks under a 1:1 slope. Further dimensions were:

$$R_0 = 8.53 \text{ m (28 ft)}; \; B_{bed} = 1.83 \text{ m (6 ft)}$$

and the experiment was run under the flow conditions:

$$\underline{d} = 0.16 \text{ m } (0.512 \text{ ft}) \quad ; \quad V^2/g\underline{d} = 0.34 \quad ; \quad C^2/g = 500$$

In the computations, the channel was assumed to have a rectangular cross-section of $B_{bed} + \underline{d} = 1.99$ m (6,5 ft) wide. Furthermore, the inflow and outflow conditions were taken the same as in the simulation of the LFM-experiments.
The velocity-distribution following from these computations and experiments is shown in fig. 9 for the second bend and the preceding straight reach. Now the deviations from the measured data are considerable even in the first part of the represented section. This is a consequence of the curved section immediately upstream, which causes deviations similar to those found in the previous cases. Thus the 'extra' shift of the velocity-maximum towards the right hand bank (being the outer bank of the preceding bend) could be explained.
Eliminating this effect, however, the agreement in the downstream part of the second bend becomes worse, the model predicting no outward shift of the velocity-maximum at all.

B. C.L. Yen's 'equilibrium bed' experiment.

C.L. Yen conducted a series of experiments in the same flume as B.C. Yen used, but he applied vertical sidewalls and a loose sand bed[13]. Under various flow conditions he determined among other things the equilibrium bed configuration, defined as the configuration of the average bed (i.e. with all irregularities like ripples and dunes smoothed out) in its final state, when variations with time no longer occur.
For one selected set of conditions, viz.:

$$R_0 = 8.53 \text{ m } (28 \text{ ft}) \quad ; \quad B = 2.36 \text{ m } (7.75 \text{ ft}) \; ;$$

$$\underline{d} = 0.12 \text{ m } (0.38 \text{ ft}) \; ; \; V^2/g\underline{d} = 0.09$$

this equilibrium bed was reproduced in concrete and subsequently experiments were conducted under the same flow conditions, apart from a correction of the longitudinal channel slope accounting for the reduction of the bed resistance due to the smaller grain roughness of the concrete bed and the absence of ripples or dunes. Unfortunately, neither the friction factor nor the corrected longitudinal slope were reported, so they had to be estimated:

$$C^2/g = 250 \; ; \; i_{bed} = g/C^2 = 4 * 10^{-3}$$

The equilibrium bed configuration, corrected for the overall channel slope, is given in fig. 10a.
The numerical simulation had to be limited to the second part of the flume, since data were available only for this section. Therefore, a non-uniform velocity-distribution was imposed at the upstream boundary. For practical purposes a parabola was chosen, somewhat resembling the measured distribution, but in principle any distribution can be chosen as long as no negative longitudinal velocities occur.
The vorticity at the upstream boundary was assumed to be zero and a linear free surface configuration was imposed at the downstream boundary, such that the measured configuration was more or less represented there.
Fig. 10b shows the velocity-distribution and fig. 10c the bed shear stress computed from these data, together with the measured values. Fig. 10d gives the measured flow direction near the bed and the computed bed shear stress direction.
Considering the velocities, the same phenomenon as in the simulation of B.C. Yen's flat bed experiment shows up a fortiori: the velocity-maximum shifts to the right hand bank as a consequence of the preceding bend. In the computations, however, this bend is absent, whence the skewness of the velocity-distribution vanishes rather quickly downstream of the inflow boundary.

A possible way to improve this upstream condition is to account for the radial flow occuring at this boundary by adopting some other boundary condition for the vorticity (e.g. a prescription of $\frac{\partial \omega}{\partial s}$ instead of ω itself), but even in that case it must be doubted whether a good connection with the bend upstream can be realized. Beyond the first part of the bend under consideration , the effect of the preceding bend is no longer identifiable and the velocity-maximum shifts to the outer bank much faster than in B.C. Yen's flat bed experiment. This is no effect of curvature, however, but rather a consequence of the bed configuration, which forces the flow to pass mainly through the deeper parts of the cross-section. This phenomenon is fairly well represented by the computations, although the velocity near the inner bank remains too high (the measured data even suggest a streamline separation from the banks).
The bed shear stress distribution shows essentially the same features as the velocity-distribution: poor agreement between measurement and computations in the upstream part, probably caused by the inadequate account of the preceding bend,and a somewhat better agreement in the downstream part, except near the inner bank. The deviations of the shear stress from the streamwise direction, however, seem to agree fairly well with the measured deviations of the velocity near the bed.
The computed free surface elevation included a transverse slope, indeed, but much smaller than the observed one (the superelevation half way along the bend was computed as about 50% of the observed value). Besides, there was a large 'scatter' in the numerical results. Since this scatter increased from the downstream edge on, the free surface computation probably was insufficiently accurate. This may be true, since the longitudinal step size was about 1.4 ft (0.43 m), which is rather large with respect to the longitudinal dimensions of the banks and the throughs (order of magnitude 5-10 ft (1.52 - 3.05 m)).

Conclusion: The results of the mathematical computations represent the experimental results rather poorly, especially when considering the transverse distribution of the depth-averaged total velocity. Only in case of a bed configuration deviating considerably from the flat bed, a better agreement can be expected.
The discrepancies in the velocity-distributions are probably caused by the influence of the banks and by the influence of the secondary flow on the main flow. There are two phenomena in this respect, viz. the transverse transport of longitudinal momentum and the "turn around" of the secondary circulation near the banks.

1. Transverse transport of longitudinal momentum.
At some distance from the banks, the transverse circulation mainly consists of the transverse velocity-component, directed outward in the upper part of the cross-section (where the higher values of the main velocity occur) and inward in the lower part (covering the lower values of the main velocity). Consequently, a net transport of longitudinal momentum in transverse direction occurs, which is not accounted for in the present computations.
In mathematical terms, actually:

$$\int_{z_b}^{z_s} v_s v_n \, dz \neq 0 \tag{193}$$

v_s and v_n being the velocity-components in streamwise and transverse direction, respectively, while from the present model it follows that:

$$\int_{z_b}^{z_s} v_s v_n \, dz \sim (z_s - z_b)\, \bar{v}_s \bar{v}_n \tag{194}$$

which vanishes, since $\bar{v}_n = 0$ by definition of the streamwise coordinates.
In the present asymptotic approach, eq. 193 represents a second

order effect, which is correct in the philosophy of this model, assuming the sidewalls not to influence the solution at some distance from these walls. Inclusion of this second order effect in the present computations proves to have a small effect upon the solution, indeed.

If, as Rozovskii suggests[6], the effect of the no-slip condition at the sidewalls on the main flow distribution and the effect of the impermeability of the wall on the distribution of the transverse velocity are included, however, the above mentioned transverse transport of longitudinal momentum becomes much more important. Then the relevant advective term in the depth-integrated streamwise equation of motion

$$\int_{z_b}^{z_s} \frac{\partial}{\partial n}(v_s v_n)\, dz \qquad (195)$$

becomes much more important as a consequence of the steep transverse gradients of the velocities near the banks. The term is positive near the inner bank and negative near the outer bank, thus causing a deceleration of the main flow in the former region and an acceleration in the latter one, as was shown for axisymmetric laminar flow by the present author[15].

Besides, the term causes an extension of the region with high velocity-gradients near the banks, such that in non-axisymmetric flows the accelerating and decelerating effects have the opportunity to spread out over an increasing region until the entire cross-section is influenced. Thus one of the basic concepts of the present model is violated and a main flow distribution is generated with a velocity maximum outward shifting.

2. The "turn around" of the transverse circulation.

Near the banks the vertical velocity-component is much larger than near the centreline, viz. of the same order of magnitude as

the transverse velocity-component [15]. Near the inner bank the vertical velocity is directed upward, causing an upward transport of "low momentum fluid" from the lower corner. In the upper part of the vertical this fluid is conveyed outward as described before.

In mathematical terms: near the banks the term:

$$\frac{\partial}{\partial z}(v_s v_z)$$

in the longitudinal momentum equation becomes a first order term. Near the inner bank it is positive in the greater part of the vertical, except near the free surface, where a negative peak occurs such that the integral value of the term vanishes. As is shown in ref. 15, this causes a deceleration of the main flow. Near the outer bank a similar reasoning leads to an acceleration of the main flow. Obviously, the turn around of the secondary circulation near the banks acts upon the main flow in the same way as the net transverse transport of longitudinal momentum, thus increasing the outward shift of the velocity-maximum.

These ideas are confirmed by experimental observations, especially in narrower channels, like Fox and Ball's [16], shown in fig. 11. It is seen that the velocity-distribution shifts to the inner bank in the first part of the bend, but after about 30^{o} the influence of the secondary circulation becomes more and more perceptible until the entire flow field is influenced in the second half of the bend.

XI. SUMMARY, CONCLUSIONS AND FURTHER RESEARCH.

Starting from a general mathematical model of steady turbulent flow, consisting of the Reynolds equations and the boundary conditions at the free and the 'no-slip' boundaries, a simplified model of shear flow in shallow curved open channels has been derived. The assumptions underlying the simplification are:

1. the shear stress tensor is related to the rate-of-strain tensor through a scalar "coefficient of turbulence viscosity", which may vary in space,
2. in a shallow river at a distance from the banks the vertical velocity-gradients dominate the horizontal ones,
3. the shear stress effects dominate the inertial (advective) effects.

The latter two assumptions only hold good if the average depth of flow is small with respect to the radius of curvature, or rather if the vertical length scale is small with respect to the horizontal one. Besides, they turn out to imply that the no-slip conditions at the sidewalls do not influence the flow pattern at larger distances from these walls.

In addition, the coefficient of turbulence viscosity is assumed to be distributed over the vertical essentially in the same way as in uniform shear flow having a logarithmic velocity-distribution. Likewise, the velocity is assumed to vanish at a prescribed level above the bed, as usual in simple uniform flow computations.

The normalized dependent variables (total pressure, velocity components) solved from the simplified system of equations and boundary conditions turn out to have the form

$$f(\xi,\eta,\zeta) = \sum_n g_n(\xi,\eta)\ h_n(\zeta) \qquad (196)$$

Hence it is possible to solve the problem in two subsequent steps:

1. determine the vertical distribution of the dependent varia-

bles (in fact: determine the functions $h_n(\zeta)$ in eq. 196)

2. integrate the whole system of equations over the depth of flow, taking account of the functions $h_n(\zeta)$ found from the first step, and solve for the depth-averaged dependent variables, or rather the functions $g_n(\xi,\eta)$ in eq. 196.

In this way the three-dimensional problem is split up into two simpler problems, one being one-dimensional, the other one being two-dimensional in the horizontal plane. The former problem can be solved analytically; the latter one requires application of procedures which have been elaborated.

Comparing the vertical distribution of the dependent variables in case of axisymmetric flow (i.e. no changes in longitudinal direction) with theoretical and experimental results obtained by other researchers, the present model turns out to be a fairly good one.

Considering the horizontal distribution of the depth-averaged variables in a curved channel without assuming axial symmetry, however, the conclusion must be less positive: experimental data are not well represented, particularly in the downstream part of the bend and downstream of it. The agreement is less for a flat bed than for a configuration with banks and troughs. The differences between the measured and the computed results may be explained qualitatively by the absence of advective effects of the secondary flow on the main flow in the present mathematical model.

Although the mathematical model has limited applicability, it shows some important features of non-axisymmetric curved flows:

1. The secondary flow 'plane' is not perpendicular to the streamwise direction, as in the case of axisymmetric flow, since both longitudinal and transverse accelerations cause a secondary flow.
2. As a consequence of the above mentioned secondary flow, the streamwise component of the bed shear stress in increased if the main flow accelerates and decreased if the main flow decelerates. The transverse component of the bed shear stress arises from the secondary flow alone; it is caused by the stream-

line curvature and directed towards the centre of curvature. Therefore, in regions of decelerating curved flow the bed shear stress vector will deviate from the streamwise direction at larger angles than in axisymmetric flow of the same curvature, while in accelerating regions the angle of deviation is smaller.

3. Even though the bed shear stress vector may deviate considerably from the stream direction, the "secondary" bed shear stress is of minor importance to the computation of the depth-averaged quantities.

Further research.

The present research as to curved river problems may be continued in two different ways:

1. It may be attempted to improve the mathematical model of the flow field by including the advective effect of the secondary flow on the main flow. To that end, the influence of the sidewalls must be taken into account, which could be done by extending the model to the sidewall regions or by correcting the present model for the most important sidewall effects in an approximative way.

The description of the flow field near the sidewalls raises many problems, physically (turbulence model) as well as mathematically (cf. the computation of laminar, axisymmetric flow [15]). Maybe it will be profitable to use a very simple turbulence model, such as the parabolic one, having a constant eddy viscosity (but then the problem is what slip-velocities must be prescribed at the walls).

Attempting to give an approximate description of the most important sidewall effects, one must have an insight into the phenomena occurring in the sidewall regions. This could be obtained by elaborating a simplified model of the flow in these regions, such as the laminar flow model or the above mentioned parabolic model.

2. Since the present model yields more satisfactory results in case of bed configurations deviating from a flat bed, it is more suitable for the prediction of the equilibrium configuration of erodible beds.

Starting from a flat bed, the velocity and bed shear stress distributions are not correct, but both act upon the bed in a correct sense, viz. in the inward direction. Confining the problem to relatively coarse sediments, such that only bed load transport will occur, and making the sidewalls impermeable to the sediment (they are not for the secondary flow!), sedimentation will be predicted near the inner wall and erosion near the outer wall, thus indicating the formation of a bank and a through, respectively. Qualitatively, this agrees with observed configurations (cf. fig. 10 a).

The actual procedure may be iterative [10] or a quasi-steady step by step procedure. Both consist of the computation of a steady state flow field followed by a bed level computation, the former trying to predict the equilibrium level directly, the latter using an extrapolation in time based on sediment transport laws. In that case the rate of sedimentation $\frac{\partial z_b}{\partial t}$ follows from the equation of continuity of the sediment:

$$(1-p)\,\frac{\partial z_b}{\partial t} + \frac{\partial S_x}{\partial x} + \frac{\partial S_y}{\partial y} = 0 \qquad (179)$$

with: p = porosity of the bed

S_x, S_y = components of the sediment transport vector in x- and y-direction, respectively.

An iterative procedure for the prediction of the equilibrium configuration of the bed is followed by Engelund[10]. Applying a mathematical model which is more simplified than the present one he obtains (after only two iterations!) a good prediction of the configuration found experimentally by Hooke in a sinusoidal channel [17].

An important problem arising in these erodible bed computations are the dynamic equations for the sediment transport components, where a problem is encountered that does not appear in "one-dimensional" sediment transport computations: the banks and troughs involve relatively steep bed slopes (i.e. much steeper than the overall channel slope), such that the component along the bed of the gravitational

force can not be neglected with respect to the other forces acting upon the bed.

XII. ACKNOWLEDGEMENTS

The theoretical part of the research was part of the research program of the Laboratory of Fluid Mechanics of the Dept. of Civil Engineering, Delft University of Technology. Besides, experiments were conducted in this laboratory by the Group of River Hydraulics of the Dept. of Civil Engineering, the results of which were kindly put at the author's disposal.
The author is greatly indebted to mr E.O.F. Calle for the great deal of mathematical work he spent to the project and he further wishes to thank Dr C. Kranenburg and Dr J.P.Th. Kalkwijk for their advice. Besides he thanks mr D.C. Post for drawing the figures and mrs A.F. van Gelder-Lensen for doing the complex typework.

XIII. REFERENCES

1. J. Boussinesq,
"Mémoire sur l'influence de frottement dans les mouvements réguliers des fluides",
§ XII- "Essai sur le mouvement permanent d'un liquide dans un canal horizontal à axe circulaire"
Journal de Mathématiques pures et appliquées,
Deuxième série, tome XIII, 1868, p. 413.

2. H.J. de Vriend,
"Literatuuroverzicht bochtstroming",
Lab. voor Vloeistofmechanica, Afd der Weg- en Waterbouwkunde,
T.H. Delft, Rapport nr R1972/1/L, 1973.

3. J. Kuipers and C.B. Vreugdenhil,
"Calculations of two-dimensional horizontal flow",
Delft Hydraulics Laboratory,
Rept S 163 pt.I, October 1973

4. P. Bradshaw,
"Calculation methods for complex flows",
Lecture notes of the VKI Lecture series 76,
"Prediction methods for turbulent flows", 1975.

5. B.E. Launder and D.B. Spalding,
"Mathematical models of turbulence",
Academic Press, London, 1972

6. I.L. Rozovskii,
"Flow of water in bends of open channels"
Israel Program for Scientific Translations,
Jerusalem, 1961.

7. B.C. Yen,
"Spiral motion of developed flow in wide curved open channels,
Symposium to Honor Professor H.A. Einstein,
June 1971 at the University of California, Berkeley
Edited by H.W. Shen, 1972

8. A.K. Ananyan,
"Fluid flow in bends of conduits"
Israel Program for Scientific Translation,
Jerusalem, 1965

9. H. Kikkawa, S. Ikeda, H. Ohkawa, Y. Kawamura.
"Secondary flow in a bend of a turbulent stream"
Transactions of the JSCE, vol. 5, 1973, p. 100

10. F. Engelund.
"Flow and bed topography in channel bends"
Proceedings of the ASCE, Jnl Hydraulics Division,
vol 100, no HY11, November 1974, p 1631.

11. S. Ikeda.
"On secondary flow and bed profile in alluvial curved open channel"
Proceedings of the XVIth Congress of the IAHR,
Sao Paulo, 1975 vol. 2, paper B-14

12. B.C. Yen, C.L. Yen.
"Water surface configuration in channel bends"
Proceedings of the ASCE, Jnl Hydraulics Division,
vol 97, no HY2, February 1971, p 303

13. C.L. Yen.
"Bed configuration and characteristics of subcritical flow in a meandering channel"
Dissertation presented to the University of Iowa, Iowa City, 1967

14. B.C. Yen.
Characteristics of subcritical flow in a meandering channel"
Institute of Hydraulic Research, University of Iowa, Iowa City, 1965.

15. H.J. de Vriend,
"Theory of viscous flow in curved shallow channels",
Communications on Hydraulics, Delft University of Technology, Dept. of Civil Engineering, Rept. 72-1, 1973.

16. J.A. Fox, D.J. Ball,
"The analysis of secondary flow in bends in open channels"
Proceedings of the Inst. of Civil Engrs., London, vol. 39, 1968, p. 467

17. R.L. Hooke,
"Shear stress and sediment distribution in a meander bend"
UNGI-report 30, University of Uppsala, Sweden, 1974.

LIST OF SYMBOLS

A	scalar viscosity-coefficient
$\underline{A}$	scalefactor of A
B	channel width
C	Chezy's constant
d	depth of flow
$\underline{d}$	vertical length scale (characteristic depth of flow)
$F = (V^2/gd\varepsilon)^{\frac{1}{2}}$	"normalized" Froudenumber
$F_1(Z)$, $F_2(Z)$	component of the vertical distribution of the secondary flow
fdev(Z)	function describing the vertical distribution of the tangent of the velocity deviation angle ϕ_{dev}
fsec(Z)	function describing the vertical distribution of the horizontal component of the secondary flow
g	acceleration due to gravity
K	transverse surface slope coefficient
k	equivalent bottom roughness
L	normalized mixing length
m'	constant in the parabolic formula for the vertical distribution of the main flow
n	coordinate along the normal lines of the depth-averaged flow field
P	scalefactor of the total pressure $p + \rho gz$
p	isotropic pressure
$\underline{p}$	normalized total pressure
$\bar{p}$	depth-averaged value of $\underline{p}$
$\underline{p}_0$, $\underline{p}_1$, ...	subfunctions in the series expansion of $\underline{p}$
$\bar{p}_0$, $\bar{p}_1$, ...	subfunctions in the series expansion of $\bar{p}$
Q	discharge
R	local radius of curvature
R_0	horizontal length scale (representative radius of curvature)
r	normalized radial coordinate in a polar coordinate system

r_i	normalized radius of curvature of the inner wall
r_n	normalized radius of curvature of the normal lines in the depth-averaged flow field
r_{n0}, r_{n1}, ...	subfunctions in the series expansion of r_n
r_o	normalized radius of curvature of the outer wall
r_s	normalized radius of curvature of the streamlines in the depth-averaged flow field
r_{s0}, r_{s1}, ...	subfunctions in the series expansion of r_s
$Re' = \rho V\underline{d}/\underline{A}$	Reynoldsnumber based on the turbulent viscosity scale
s	coordinate along the streamlines of the depth-averaged flow field
S_x, S_y	component of the sediment transport in x-(y-)direction
$\bar{T}_s$	streamwise inertial terms in the depth-averaged computation
$\bar{T}_n$	transverse inertial terms in the depth-averaged computation
$\bar{T}_\xi$	inertial terms in ξ-direction in depth-averaged computation
$\bar{T}_{\xi 0}$, $\bar{T}_{\xi 1}$,...	subfunctions in the series expansion of $\bar{T}_\xi$
$\bar{T}_\eta$	inertial terms in η-direction in depth-averaged computation
$\bar{T}_{\eta 0}$, $\bar{T}_{\eta 1}$,...	subfunctions in the series expansion of $\bar{T}_\eta$
U	scalefactor of the velocity-component in x-direction
u	normalized velocity-component in ξ-direction
u'	normalized total horizontal velocity
$\bar{u}$, $\bar{u}'$	depth-averaged value of u, u'
$\tilde{u}$	depth-averaged factor in the ξ-component of secondary flow
u_0, u_1, ...	subfunctions in the series expansion of u
u_0', u_1', ...	subfunctions in the series expansion of u'
$\bar{u}_0$, $\bar{u}_1$, ...	subfunctions in the series expansion of $\bar{u}$
$\bar{u}'$, $\bar{u}'$, ...	subfunctions in the series expansion of $\bar{u}'$

$\tilde{u}_1$	equivalent of $\tilde{u}$ in the solution of the first order system
V	scale-factor of the velocity-component in y-direction and of the horizontal velocities
v	normalized velocity-component in η-direction
$\bar{v}$	depth-averaged value of v
$\tilde{v}$	depth-averaged factor in the η-component of secondary flow
$v_0, v_1, \ldots$	subfunctions in the series expansion of v
$\bar{v}_0, \bar{v}_1, \ldots$	subfunctions in the series expansion of $\bar{v}$
$\tilde{v}_1$	equivalent of $\tilde{v}$ in the solution of the first order system
v_n	velocity-component along the normal lines of the depth-averaged flow field
v_s	velocity-component along the stramlines of the depth-averaged flow field
v_{tot}	total horizontal velocity
v_x	velocity-component in x-direction
v_y	velocity-component in y-direction
v_z	velocity-component in z-direction
W	scalefactor of the vertical velocity-component
w	normalized vertical velocity-component
w_0, w_1	subfunctions in the series expansion of w
X	scalefactor of the x-coordinate
x	horizontal coordinate in a Cartesian system
Y	scalefactor of the y-coordinate
y	horizontal coordinate in a Cartesian system
Z	in chapter III: scalefactor of the z-coordinate elsewhere: $Z = \frac{\zeta - \zeta_s}{\zeta_s - \zeta_b}$
$Z' = \frac{\zeta'}{\zeta_s - \zeta_b}$	
$Z_0, Z_1, \ldots$	subfunctions in the series expansion of Z
$Z', Z', \ldots$	subfunctions in the series expansion of Z'
z	vertical coordinate

z_b	bed level
z_s	free surface elevation
α	normalized viscosity-coefficient A
α_t	normalized coefficient of turbulence viscosity
$\alpha_{t0}, \alpha_{t1}, \ldots$	subfunctions in the series expansion of α_t
δ	thickness of the layer between the bed and the level of zero "secondary" shear stress
Δ	longitudinal slope of the energy-line in the channel-axis
$\varepsilon = \underline{d}/R_0$	perturbation parameter
ε'	small parameter (undefined)
ζ	normalized vertical coordinate
ζ'	normalized level near the bed where the velocities vanish
$\zeta'_0, \zeta'_1, \ldots$	subfunctions in the series expansion of ζ'
ζ_b	normalized bed level
ζ_s	normalized free surface level
$\zeta_{s0}, \zeta_{s1}, \ldots$	subfunctions in the series expansion of ζ_s
η	normalized y-coordinate
κ	Von Kármán's constant
ν	kinematical viscosity of the fluid
ξ	normalized x-coordinate
ρ	mass density of the fluid
$\sigma_{xx}, \sigma_{yy}, \sigma_{zz}$	normal stress components of the stress-tensor
τ_{nbed}	normalized bed shear stress component in n-direction
$\tau_{n\zeta}$	normalized shear stress component in n-direction
τ_{sbed}	normalized bed shear stress component in s-direction
$\tau_{s\zeta}$	normalized shear stress component in s-direction
$\tau_{xy}, \tau_{yz}, \tau_{zx}$	shear stress components of the stress-tensor
Φ	streamfunction of the depth-averaged horizontal velocities
$\Phi_0, \Phi_1, \ldots$	subfunctions in the series expansion of Φ

ϕ	tangential coordinate in polar coordinate-system
ϕ_v	deviation angle of the velocity-vector from the s-direction
ϕ_τ	deviation angle of the bed shear stress from the s-direction
ω	vorticity of the depth-averaged velocity-field
$\omega_0, \omega_1, \ldots$	subfunctions in the series expansion of ω

APPENDIX I: Asymptotic expansion of the boundary conditions.

Suppose a function f(x) must satisfy at $x=x_b$ the boundary condition:

$$f(x)\Big|_{x_b} = f_b \tag{I.1}$$

If f(x), f_b and x_b can be expanded in a power series of the small parameter ε, such that:

$$f(x) = f_0(x) + \varepsilon f_1(x) + \varepsilon^2 f_2(x) + ... \tag{I.2}$$

$$f_b = f_{b0} + \varepsilon f_{b1} + \varepsilon^2 f_{b2} + ... \tag{I.3}$$

$$x_b = x_{b0} + \varepsilon x_{b1} + \varepsilon^2 x_{b2} + ... \tag{I.4}$$

what are the boundary conditions to be imposed on the subfunctions $f_i(x)$ then? Making use of the series expansions I.2-I.4, condition I.1. can be written:

$$\left[f_0(x) + \varepsilon f_0(x) + \varepsilon^2 f_0(x) + ...\right]_{x_{b0} + \varepsilon x_{b1} + \varepsilon^2 x_{b2} + ...} =$$

$$f_{b0} + \varepsilon f_{b1} + \varepsilon^2 f_{b2} + ... \tag{I.5}$$

Expanding the left hand part of this equation in a Taylor-series around x_{b0} yields:

$$\left[f_0 + \varepsilon f_1 + \varepsilon^2 f_2 + ...\right]_{x_{b0}} + (\varepsilon x_{b1} + \varepsilon^2 x_{b2} + ...) *$$

$$\left[\frac{df_0}{dx} + \varepsilon\frac{df_1}{dx} + \varepsilon^2 \frac{df_2}{dx} + ...\right]_{x_{b0}} + \frac{1}{2!}(\varepsilon x_1 + \varepsilon^2 x_2 + ...)^2 *$$

$$\left[\frac{d^2f_0}{dx^2} + \varepsilon\frac{d^2f_1}{dx^2} + \varepsilon^2 \frac{d^2f_2}{dx^2} + ...\right]_{x_{b0}} = f_{b0} + \varepsilon f_{b1} + \varepsilon^2 f_{b2} + ... \tag{I.6}$$

Collecting the terms with the same power of ε and putting each of these groups of terms equal to zero yields the conditions to be imposed on the various subfunctions:

$$f_0(x)\Big|_{x_{b0}} = f_{b0} \tag{I.7}$$

$$f_1(x)\Big|_{x_{b0}} = f_{b1} - x_{b1}\,\frac{df_0}{dx}\Big|_{x_{b0}} \tag{I.8}$$

$$f_2(x)\Big|_{x_{b0}} = f_{b2} - x_{b2}\,\frac{df_0}{dx}\Big|_{x_{b0}} - x_{b1}\,\frac{df_1}{dx}\Big|_{x_{b0}} + - \frac{1}{2}\,x_1^2\,\frac{d^2f_0}{dx^2}\Big|_{x_{b0}} \tag{I.9}$$

etcetera.

Each of the boundary conditions of the normalized system (see conds. 32-35 and cond. 48) has been treated this way, yielding the following results:

1. Condition 33: $w\big|_{\zeta_s} = u\big|_{\zeta_s}\,\frac{\partial\zeta_s}{\partial\xi} + v\big|_{\zeta_s}\,\frac{\partial\zeta_s}{\partial\eta}$

$$w_0\big|_{\zeta_{s0}} = u_0\big|_{\zeta_{s0}}\,\frac{\partial\zeta_{s0}}{\partial\xi} + v_0\big|_{\zeta_{s0}}\,\frac{\partial\zeta_{s0}}{\partial\eta} \tag{I.10}$$

$$w_1\big|_{\zeta_{s0}} = (u_1 + \zeta_{s1}\,\frac{\partial u_0}{\partial\zeta})\Big|_{\zeta_{s0}}\,\frac{\partial\zeta_{s0}}{\partial\xi} + u_0\big|_{\zeta_{s0}}\,\frac{\partial\zeta_{s1}}{\partial\xi} + + (v_1 + \zeta_{s1}\,\frac{\partial v_0}{\partial\zeta})\Big|_{\zeta_{s0}}\,\frac{\partial\zeta_{s0}}{\partial\eta} + v_0\big|_{\zeta_{s0}}\,\frac{\partial\zeta_{s1}}{\partial\eta} - \zeta_{s1}\,\frac{\partial w_0}{\partial\zeta}\Big|_{\zeta_{s0}} \tag{I.11}$$

2. Condition 34: $p\big|_{\zeta_s} = \frac{\zeta_s}{F^2}$

$$p_0\big|_{\zeta_{s0}} = \frac{\zeta_{s0}}{F^2} \tag{I.12}$$

$$p_1\big|_{\zeta_{s0}} = \frac{\zeta_{s1}}{F^2} - \zeta_{s1}\,\frac{\partial p_0}{\partial \zeta}\Big|_{\zeta_{s0}} \tag{I.13}$$

$$p_2\big|_{\zeta_{s0}} = \frac{\zeta_{s2}}{F^2} - \zeta_{s2}\,\frac{\partial p_0}{\partial \zeta}\Big|_{\zeta_{s0}} - \zeta_{s1}\,\frac{\partial p_1}{\partial \zeta}\Big|_{\zeta_{s0}} - \frac{1}{2}\,\zeta_{s1}^2\,\frac{\partial^2 p_0}{\partial \zeta^2}\Big|_{\zeta_{s0}} \tag{I.14}$$

3. Condition 35: $\alpha\left(\frac{\partial u}{\partial \zeta} + \varepsilon^2\,\frac{\partial w}{\partial \xi}\right)\Big|_{\zeta_s} = \alpha\left(\frac{\partial v}{\partial \zeta} + \varepsilon^2\,\frac{\partial w}{\partial \eta}\right)\Big|_{\zeta_s} = 0$ (I.15)

$$\left(\alpha_0\,\frac{\partial u_0}{\partial \zeta}\right)\Big|_{\zeta_{s0}} = 0 \tag{I.16}$$

$$\left(\alpha_0\,\frac{\partial u_1}{\partial \zeta} + \alpha_1\,\frac{\partial u_0}{\partial \zeta}\right)\Big|_{\zeta_{s0}} = -\,\zeta_{s1}\,\frac{\partial}{\partial \zeta}\left(\alpha_0\,\frac{\partial u_0}{\partial \zeta}\right)\Big|_{\zeta_{s0}} \tag{I.17}$$

$$\begin{aligned}\left(\alpha_0\,\frac{\partial u_2}{\partial \zeta} + \alpha_1\,\frac{\partial u_1}{\partial \zeta} + \alpha_2\,\frac{\partial u_0}{\partial \zeta}\right)\Big|_{\zeta_{s0}} &= -\left(\alpha_0\,\frac{\partial w_0}{\partial \xi}\right)\Big|_{\zeta_{s0}} + \\ &- \zeta_{s2}\,\frac{\partial}{\partial \zeta}\left(\alpha_0\,\frac{\partial u_0}{\partial \zeta}\right)\Big|_{\zeta_{s0}} - \zeta_{s1}\,\frac{\partial}{\partial \zeta}\left(\alpha_1\,\frac{\partial u_0}{\partial \zeta} + \alpha_0\,\frac{\partial u_1}{\partial \zeta}\right)\Big|_{\zeta_{s0}} + \\ &- \frac{1}{2}\,\zeta_{s1}^2\,\frac{\partial^2}{\partial \zeta^2}\left(\alpha_0\,\frac{\partial u_0}{\partial \zeta}\right)\Big|_{\zeta_{s0}}\end{aligned} \tag{I.18}$$

Similar conditions hold for the subfunctions of $\alpha\left(\frac{\partial v}{\partial \zeta} + \varepsilon^2\,\frac{\partial w}{\partial \eta}\right)$.

4. Condition 48: $u\big|_{\zeta_b + \zeta'} = v\big|_{\zeta_b + \zeta'} = 0$ with $\zeta' = (\zeta_s - \zeta_b)\,\exp\left(-1 - \frac{\kappa C}{\sqrt{g}}\right)$

(I.19)

$$u_0\Big|_{\zeta_b + \zeta_0'} = 0$$

(I.20)

$$u_1\Big|_{\zeta_b + \zeta_0'} = -\frac{\zeta_{s1}}{\zeta_{s0} - \zeta_b}\,\zeta_0'\,\frac{\partial u_0}{\partial \zeta}\Big|_{\zeta_b + \zeta_0'}$$

(I.21)

$$u_2\Big|_{\zeta_b + \zeta_0'} = -\frac{\zeta_{s2}}{\zeta_{s0} - \zeta_b}\,\zeta_0'\,\frac{\partial u_0}{\partial \zeta}\Big|_{\zeta_b + \zeta_0'} + \left\{-\frac{\zeta_{s1}}{\zeta_{s0} - \zeta_b}\,\zeta_0'\,\frac{\partial u_1}{\partial \zeta} - \frac{\zeta_{s1}^2}{2(\zeta_{s0} - \zeta_b)^2}\,\zeta_0'\,\frac{\partial^2 u_0}{\partial \zeta^2}\right\}_{\zeta_b + \zeta_0'}$$

Similar conditions hold for the subfunctions of v and w.

APPENDIX II: Asymptotic expansion of α_t.

The expression adopted for the eddy viscosity was (see eq. 42):

$$\alpha_t = -\kappa^2 \frac{\zeta - \zeta_s}{\zeta_s - \zeta_b} (\zeta-\zeta_b)^2 \{ (\frac{\partial u}{\partial \zeta})^2 + (\frac{\partial v}{\partial \zeta})^2 \}^{\frac{1}{2}}$$

Using the series expansions:

$$(\frac{\partial u}{\partial \zeta})^2 = (\frac{\partial u_0}{\partial \zeta})^2 + 2\varepsilon \frac{\partial u_0}{\partial \zeta} \frac{\partial u_1}{\partial \zeta} + \varepsilon^2 \{2 \frac{\partial u_0}{\partial \zeta} \frac{\partial u_2}{\partial \zeta} + (\frac{\partial u_1}{\partial \zeta})^2\} + ...$$

$$(\frac{\partial v}{\partial \zeta})^2 = (\frac{\partial v_0}{\partial \zeta}) + 2\varepsilon \frac{\partial v_0}{\partial \zeta} \frac{\partial v_1}{\partial \zeta} + \varepsilon^2 \{2 \frac{\partial v_0}{\partial \zeta} \frac{\partial v_2}{\partial \zeta} + (\frac{\partial v_1}{\partial \zeta})^2\} + ...$$

$$\{ (\frac{\partial u}{\partial \zeta})^2 + (\frac{\partial v}{\partial \zeta})^2 \}^{\frac{1}{2}} = \{ (\frac{\partial u_0}{\partial \zeta})^2 + (\frac{\partial v_0}{\partial \zeta})^2 \}^{\frac{1}{2}} \Big[1 + \varepsilon \frac{\frac{\partial u_0}{\partial \zeta} \frac{\partial u_1}{\partial \zeta} + \frac{\partial v_0}{\partial \zeta} \frac{\partial v_1}{\partial \zeta}}{(\frac{\partial u_0}{\partial \zeta})^2 + (\frac{\partial v_0}{\partial \zeta})^2} +$$

$$+ \varepsilon^2 \frac{\frac{\partial u_0}{\partial \zeta} \frac{\partial u_2}{\partial \zeta} + \frac{\partial v_0}{\partial \zeta} \frac{\partial v_2}{\partial \zeta}}{(\frac{\partial u_0}{\partial \zeta})^2 + (\frac{\partial v_0}{\partial \zeta})^2} + \frac{\varepsilon^2}{2} \frac{(\frac{\partial u_1}{\partial \zeta})^2 + (\frac{\partial v_1}{\partial \zeta})^2}{(\frac{\partial u_0}{\partial \zeta})^2 + (\frac{\partial v_0}{\partial \zeta})^2} + ...\Big]$$

$$\frac{\zeta - \zeta_s}{\zeta_s - \zeta_b} = \frac{\zeta - \zeta_{s0} - \varepsilon\zeta_{s1} + ...}{\zeta_{s0} + \varepsilon\zeta_{s1} + ...} = \frac{\zeta - \zeta_{s0}}{\zeta_{s0} - \zeta_b} - \varepsilon \frac{\zeta_{s1}}{\zeta_{s0} - \zeta_b} \frac{\zeta - \zeta_b}{\zeta_{s0} - \zeta_b} +$$

$$- \varepsilon^2 \{ \frac{\zeta_{s2}}{\zeta_{s0} - \zeta_b} - \frac{\zeta_{s1}^2}{(\zeta_{s0} - \zeta_b)^2} \} \frac{\zeta - \zeta_b}{\zeta_{s0} - \zeta_b} + ...$$

the subfunctions of α_t turn out to be:

$$\alpha_{t0} = -\kappa^2 \frac{\zeta - \zeta_{s0}}{\zeta_{s0} - \zeta_b} (\zeta-\zeta_b)^2 \{(\frac{\partial u_0}{\partial \zeta})^2 + (\frac{\partial v_0}{\partial \zeta})^2\}^{\frac{1}{2}} \qquad \text{(II.1)}$$

$$\alpha_{t1} = -\kappa^2 \frac{\zeta - \zeta_{s0}}{\zeta_{s0} - \zeta_b} (\zeta-\zeta_b)^2 \frac{\frac{\partial u_0}{\partial \zeta}\frac{\partial u_1}{\partial \zeta} + \frac{\partial v_0}{\partial \zeta}\frac{\partial v_1}{\partial \zeta}}{\{(\frac{\partial u_0}{\partial \zeta})^2 + (\frac{\partial v_0}{\partial \zeta})^2\}^{\frac{1}{2}}} +$$

$$+ \kappa^2 \frac{\zeta_{s1}}{(\zeta_{s0} - \zeta_b)^2} (\zeta-\zeta_b)^3 \{(\frac{\partial u_0}{\partial \zeta})^2 + (\frac{\partial v_0}{\partial \zeta})^2\}^{\frac{1}{2}} \qquad \text{(II.2)}$$

$$\alpha_{t2} = -\kappa^2 \frac{\zeta - \zeta_{s0}}{\zeta_{s0} - \zeta_b} (\zeta-\zeta_b)^2 \frac{\frac{\partial u_0}{\partial \zeta}\frac{\partial u_2}{\partial \zeta} + \frac{\partial v_0}{\partial \zeta}\frac{\partial v_2}{\partial \zeta} + \frac{1}{2}(\frac{\partial u_1}{\partial \zeta})^2 + \frac{1}{2}(\frac{\partial v_1}{\partial \zeta})^2}{\{(\frac{\partial u_0}{\partial \zeta})^2 + (\frac{\partial v_0}{\partial \zeta})^2\}^{\frac{1}{2}}} +$$

$$+ \kappa^2 \frac{\zeta_{s1}}{(\zeta_{s0} - \zeta_b)^2} (\zeta-\zeta_b)^3 \frac{\frac{\partial u_1}{\partial \zeta}\frac{\partial u_1}{\partial \zeta} + \frac{\partial v_0}{\partial \zeta}\frac{\partial v_1}{\partial \zeta}}{\{(\frac{\partial u_0}{\partial \zeta})^2 + (\frac{\partial v_0}{\partial \zeta})^2\}^{\frac{1}{2}}} +$$

$$+ \kappa^2 \{\frac{\zeta_{s2}}{(\zeta_{s0} - \zeta_b)^2} - \frac{\zeta_{s1}^2}{(\zeta_{s0} - \zeta_b)^3}\} (\zeta-\zeta_b)^3 \{(\frac{\partial u_0}{\partial \zeta})^2 + (\frac{\partial v_0}{\partial \zeta})^2\}^{\frac{1}{2}}$$

(II.3)

etcetera.

APPENDIX III: Asymptotic expansion of depth-averaged quantities.

Let $\bar{f}$ be the depth-average of a function $f(\zeta)$, defined by:

$$\bar{f} = \frac{1}{\zeta_s - \zeta_b} \int_{\zeta_b}^{\zeta_s} f(\zeta)\, d\zeta \qquad \text{(III.1)}$$

how are the subfunctions of the asymptotic expansion

$$\bar{f} = \bar{f}_0 + \varepsilon\bar{f}_1 + \varepsilon^2\bar{f}_2 + ... \qquad \text{(III.2)}$$

then defined?
Substituing the series expansions

$$\zeta_s = \zeta_{s0} + \varepsilon\zeta_{s1} + \varepsilon^2\zeta_{s2} + ... \qquad \text{(III.3)}$$

$$f(\zeta) = f_0(\zeta) + \varepsilon f_1(\zeta) + \varepsilon^2 f_2(\zeta) + ... \qquad \text{(III.4)}$$

and expansion III.2 into definition III.1 multiplied by $(\zeta_s - \zeta_b)$ yields:

$$(\zeta_{s0} + \varepsilon\zeta_{s1} + \varepsilon^2\zeta_{s2} + ...)(\bar{f}_0 + \varepsilon\bar{f}_1 + \varepsilon^2\bar{f}_2 + ...) =$$

$$\zeta_{s0} + \varepsilon\zeta_{s1} + \varepsilon^2\zeta_{s2} + ... \int_{\zeta_b}^{} (f_0 + \varepsilon f_1 + \varepsilon^2 f_2 + ...)\, d\zeta \qquad \text{(III.5)}$$

The right hand part of this equation can be expanded in a Taylor-series around $\zeta=\zeta_{s0}$, such that:

$$\int_{\zeta_b}^{\zeta_s} (f_0 + \varepsilon f_1 + \varepsilon^2 f_2 + \ldots)\, d\zeta = \int_{\zeta_b}^{\zeta_{s0}} (f_0 + \varepsilon f_1 + \varepsilon^2 f_2 + \ldots)\, d\zeta +$$

$$+ (\varepsilon\zeta_{s1} + \varepsilon^2\zeta_{s2} + \ldots)(f_0 + \varepsilon f_1 + \varepsilon^2 f_2 + \ldots\ldots)\Big|_{\zeta_{s0}} +$$

$$+ \frac{1}{2!}(\varepsilon\zeta_{s1} + \varepsilon^2\zeta_{s2} + \ldots)^2 \left(\frac{df_0}{d\zeta} + \varepsilon\frac{df_1}{d\zeta} + \varepsilon^2\frac{df_2}{d\zeta} + \ldots\right)\Big|_{\zeta_{s0}}$$

(III.6)

Substitution of III.6 into III.5 yields:

$$(\zeta_{s0} - \zeta_b)\ \bar{f}_0 + \varepsilon\{(\zeta_{s0} - \zeta_b)\ \bar{f}_1 + \zeta_{s1}\ \bar{f}_0\} + \varepsilon^2\{(\zeta_{s0} - \zeta_b)\ \bar{f}_2 + \zeta_{s1}\bar{f}_1 +$$

$$+ \zeta_{s2}\bar{f}_0\} + \ldots\ldots =$$

$$= \int_{\zeta_b}^{\zeta_{s0}} f_0\, d\zeta + \varepsilon\{\int_{\zeta_b}^{\zeta_{s0}} f_1\, d\zeta + \zeta_{s1}\, f_0\Big|_{\zeta_{s0}}\} +$$

$$+ \varepsilon^2\{\int_{\zeta_b}^{\zeta_{s0}} f_2\, d\zeta + \zeta_{s1}\, f_1\Big|_{\zeta_{s0}} + \zeta_{s2}\, f_0\Big|_{\zeta_{s0}} +$$

$$+ \frac{1}{2}\zeta_{s1}^2 \frac{df_0}{d\zeta}\Big|_{\zeta_{s0}}\} + \ldots\ldots$$

(III.7)

Consequently:

$$\bar{f}_0 = \frac{1}{\zeta_{s0} - \zeta_b} \int_{\zeta_b}^{\zeta_{s0}} f_0\, d\zeta$$

(III.8)

$$\bar{f}_1 = \frac{1}{\zeta_{s0} - \zeta_b} \int_{\zeta_b}^{\zeta_{s0}} f_1 \, d\zeta + \frac{\zeta_{s1}}{\zeta_{s0} - \zeta_b} \left(f_0\Big|_{\zeta_{s0}} - \bar{f}_0\right) \tag{III.9}$$

$$\bar{f}_2 = \frac{1}{\zeta_{s0} - \zeta_b} \int_{\zeta_b}^{\zeta_{s0}} f_2 \, d\zeta + \frac{\zeta_{s1}}{\zeta_{s0} - \zeta_b} \left(f_1\Big|_{\zeta_{s0}} - \bar{f}_1\right) +$$

$$+ \frac{\zeta_{s2}}{\zeta_{s0} - \zeta_b} \left(f_0\Big|_{\zeta_{s0}} - \bar{f}_0\right) + \frac{1}{2} \frac{\zeta_{s1}^2}{\zeta_{s0} - \zeta_b} \frac{df_0}{d\zeta}\Big|_{\zeta_{s0}} \tag{III.10}$$

etcetera.

APPENDIX VI: Radius of curvature of streamlines and normal lines in a two-dimensional flow field.

Let $\vec{u}' = (u,v)$ be a two-dimensional flow field in which u and v denote the components of the velocity-vector $\vec{u}'$ in two orthogonal directions ξ and η, respectively, then the streamlines of this flow field are defined by:

$$\frac{d\eta}{d\xi} = \frac{v}{u} \tag{IV.1}$$

So: $$\frac{d}{d\xi}\left(\frac{d\eta}{d\xi}\right) = \frac{d}{d\xi}\left(\frac{v}{u}\right) = \frac{1}{u^2}\left(u\,\frac{dv}{d\xi} - v\,\frac{du}{d\xi}\right) \tag{IV.2}$$

Since: $$\frac{d}{d\xi} = \frac{\partial}{\partial\xi} + \frac{d\eta}{d\xi}\frac{\partial}{\partial\eta} = \frac{\partial}{\partial\xi} + \frac{v}{u}\frac{\partial}{\partial\eta} \tag{IV.3}$$

equation IV.2 can be written:

$$\frac{d^2\eta}{d\xi^2} = \frac{1}{u^2}\left(u\,\frac{\partial v}{\partial\xi} + v\,\frac{\partial v}{\partial\eta} - v\,\frac{\partial u}{\partial\xi} - \frac{v^2}{u}\,\frac{\partial u}{\partial\eta}\right) \tag{IV.4}$$

Defining the radius of curvature r_s of a streamline by:

$$\frac{1}{r_s} = \frac{\frac{d^2\eta}{d\xi^2}}{\{1 + (\frac{d\eta}{d\xi})^2\}^{3/2}} \tag{IV.5}$$

it follows from IV.1 and IV.4:

$$\frac{1}{r_s} = \frac{1}{u^3}\left(u^2\,\frac{\partial v}{\partial\xi} + uv\,\frac{\partial v}{\partial\eta} - uv\,\frac{\partial u}{\partial\xi} - v^2\,\frac{\partial u}{\partial\eta}\right)\left\{1 + \frac{v^2}{u^2}\right\}^{-3/2} \tag{IV.6}$$

So if $u' = \sqrt{(u^2 + v^2)}$:

$$\frac{1}{r_s} = \frac{1}{u'^3}\left(u^2 \frac{\partial v}{\partial \xi} + uv \frac{\partial v}{\partial \eta} - uv \frac{\partial u}{\partial \xi} - v^2 \frac{\partial u}{\partial \eta}\right) \qquad \text{(IV.7)}$$

The normal lines of the flow field are defined by:

$$\frac{d\eta}{d\xi} = -\frac{u}{v} \qquad \text{(IV.8)}$$

So: $$\frac{d}{d\xi}\left(\frac{d\eta}{d\xi}\right) = -\frac{1}{v^2}\left(v \frac{du}{d\xi} - u \frac{dv}{d\xi}\right) \qquad \text{(IV.9)}$$

Since: $$\frac{d}{d\xi} = \frac{\partial}{\partial \xi} + \frac{d\eta}{d\xi}\frac{\partial}{\partial \eta} = \frac{\partial}{\partial \xi} - \frac{u}{v}\frac{\partial}{\partial \eta} \qquad \text{(IV.10)}$$

equation IV.9 can be written:

$$\frac{d^2\eta}{d\xi^2} = -\frac{1}{v^2}\left(v \frac{\partial u}{\partial \xi} - u \frac{\partial u}{\partial \eta} - u \frac{\partial v}{\partial \xi} + \frac{u^2}{v}\frac{\partial v}{\partial \eta}\right) \qquad \text{(IV.11)}$$

Defining the radius of curvature of the normal lines by:

$$\frac{1}{r_n} = \frac{\frac{d^2\eta}{d\xi^2}}{\{1 + (\frac{d\eta}{d\xi})^2\}^{3/2}} \qquad \text{(IV.12)}$$

it follows from IV.8 and IV.11:

$$\frac{1}{r_n} = \frac{1}{u'^3}\left(-v^2 \frac{\partial u}{\partial \xi} + uv \frac{\partial u}{\partial \eta} + uv \frac{\partial v}{\partial \xi} - u^2 \frac{\partial v}{\partial \eta}\right) \qquad \text{(IV.13)}$$

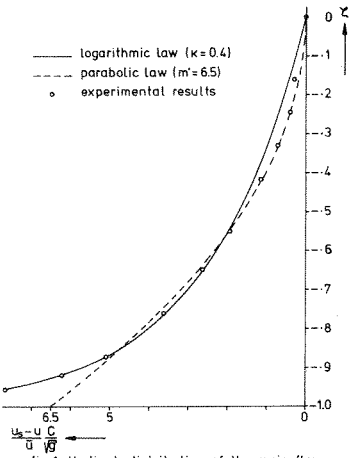

fig.1. Vertical distribution of the main flow (after Engelund[10])

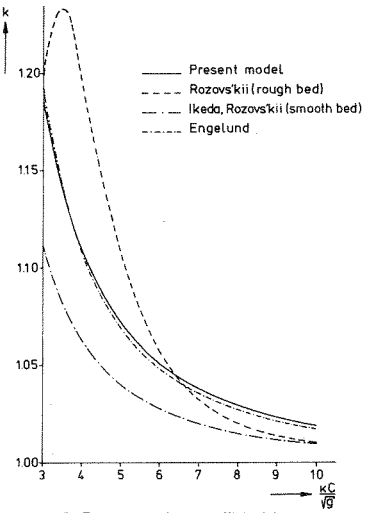

fig.5. Transverse slope coefficient k as a function of the friction factor

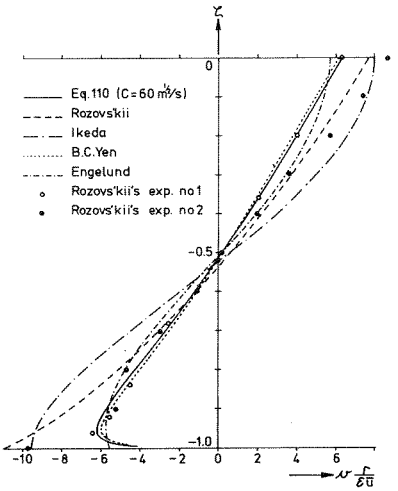

fig. 2.a. Vertical distribution of the transverse velocity in case of a smooth bed (partly after B.C. Yen[7])

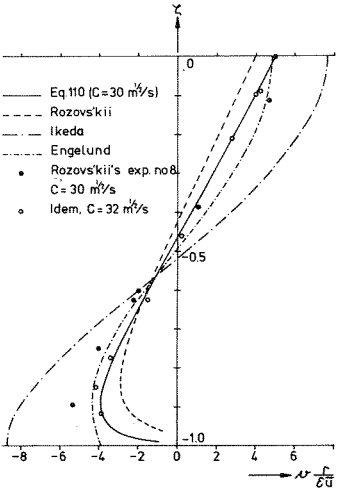

fig. 2.b. Vertical distribution of the transverse velocity in case of a rough bed

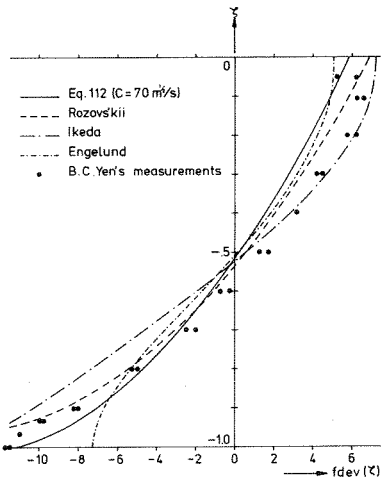

fig.3.a. Vertical distribution of the tangent of the velocity-vector deviation angle (smooth bed)

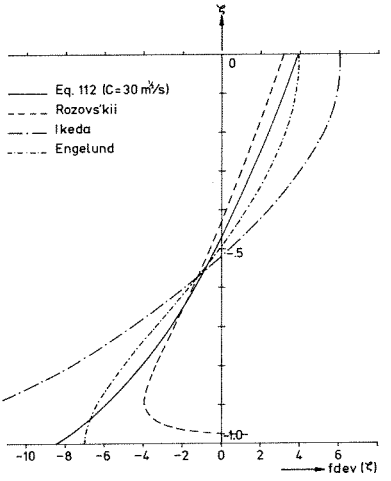

fig.3.b. Vertical distribution of the tangent of the velocity-vector deviation angle (rough bed)

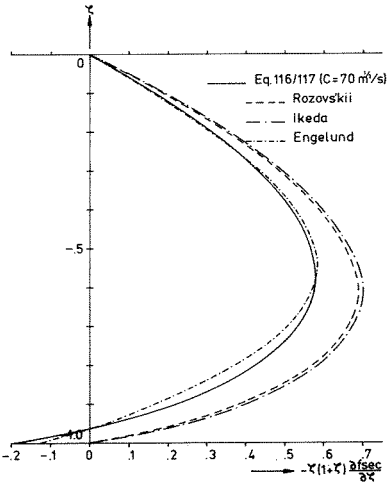

fig.4.a. Vertical distribution of the "secondary" shear stress in case of a smooth bed

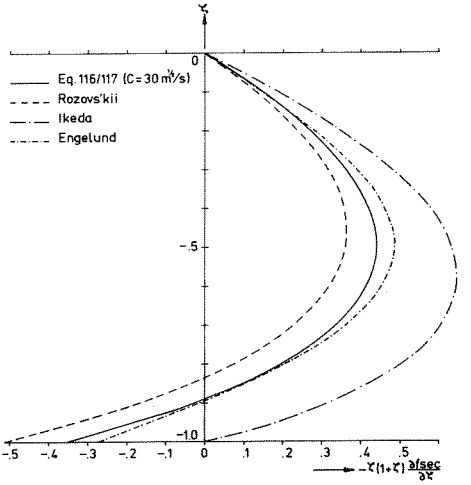

fig.4.b. Vertical distribution of the "secondary" shear stress in case of a rough bed

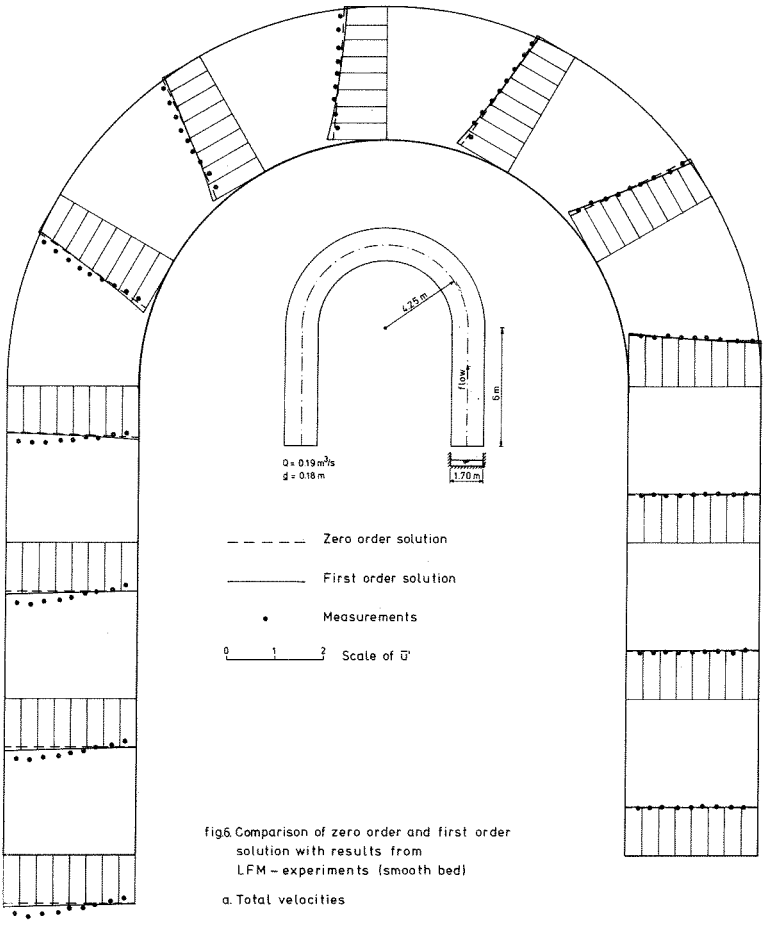

fig.6. Comparison of zero order and first order solution with results from LFM – experiments (smooth bed)

a. Total velocities

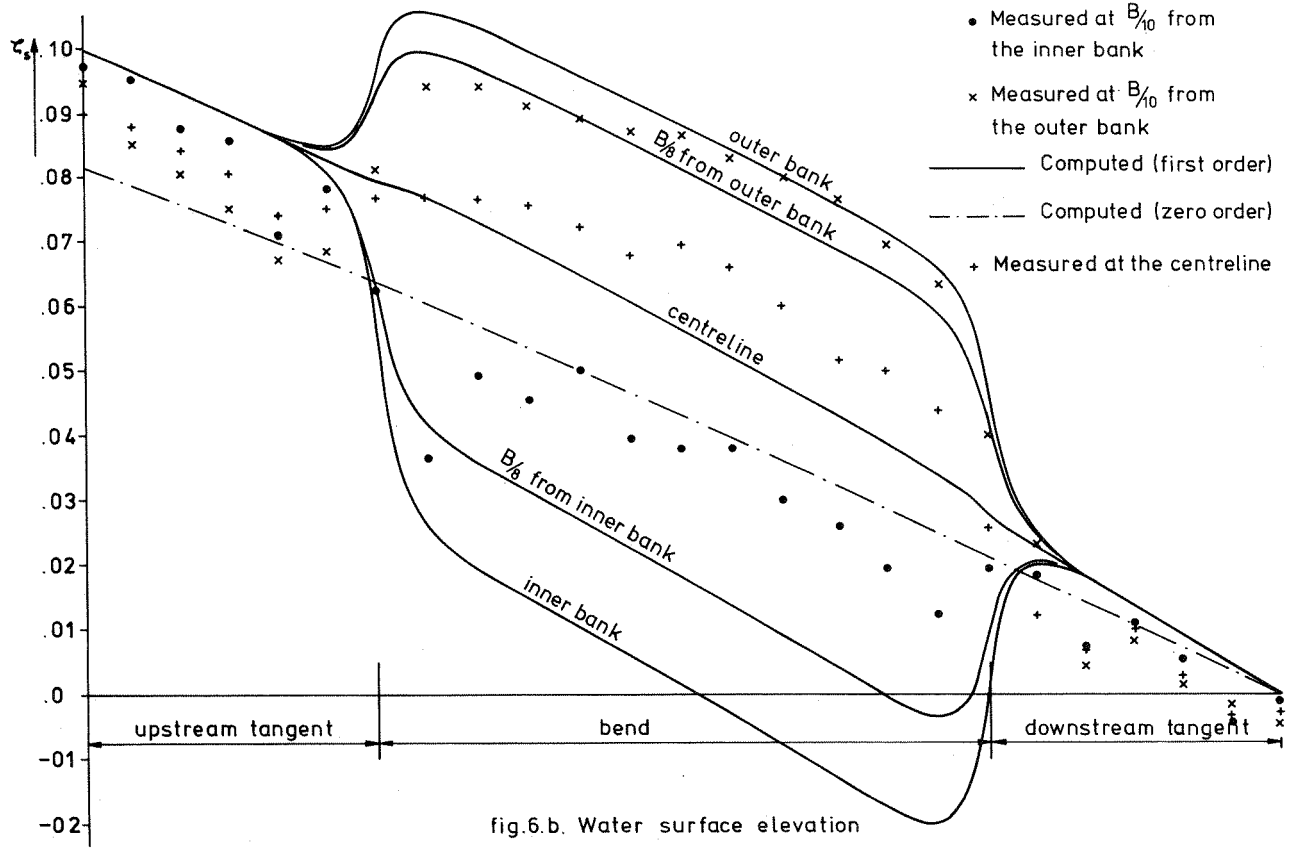

fig.6.b. Water surface elevation

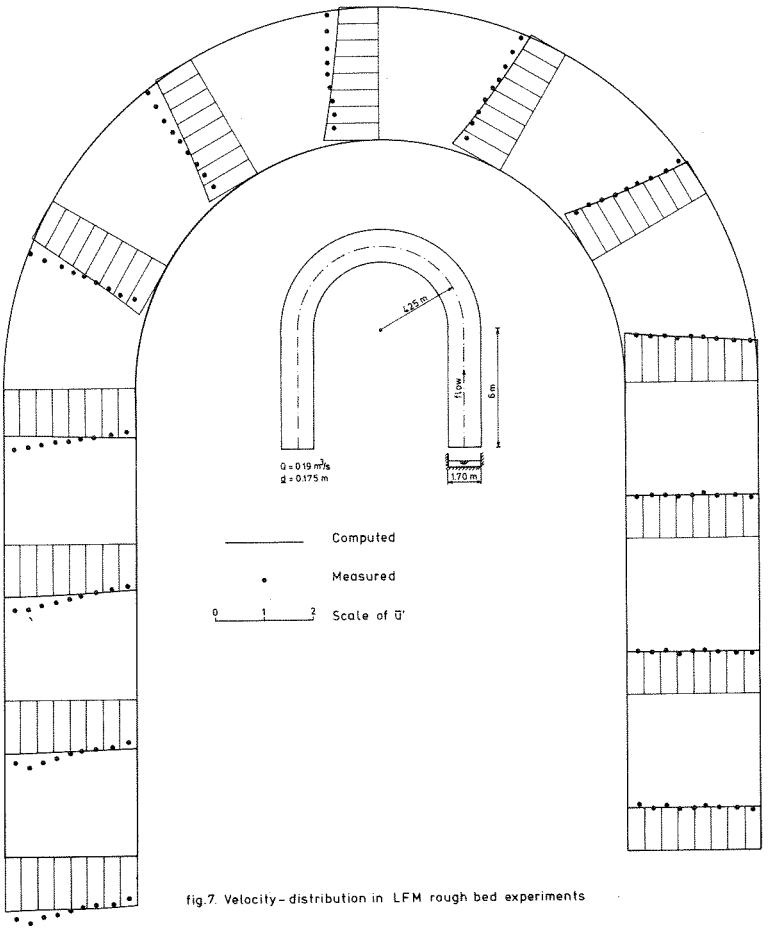

fig.7. Velocity-distribution in LFM rough bed experiments

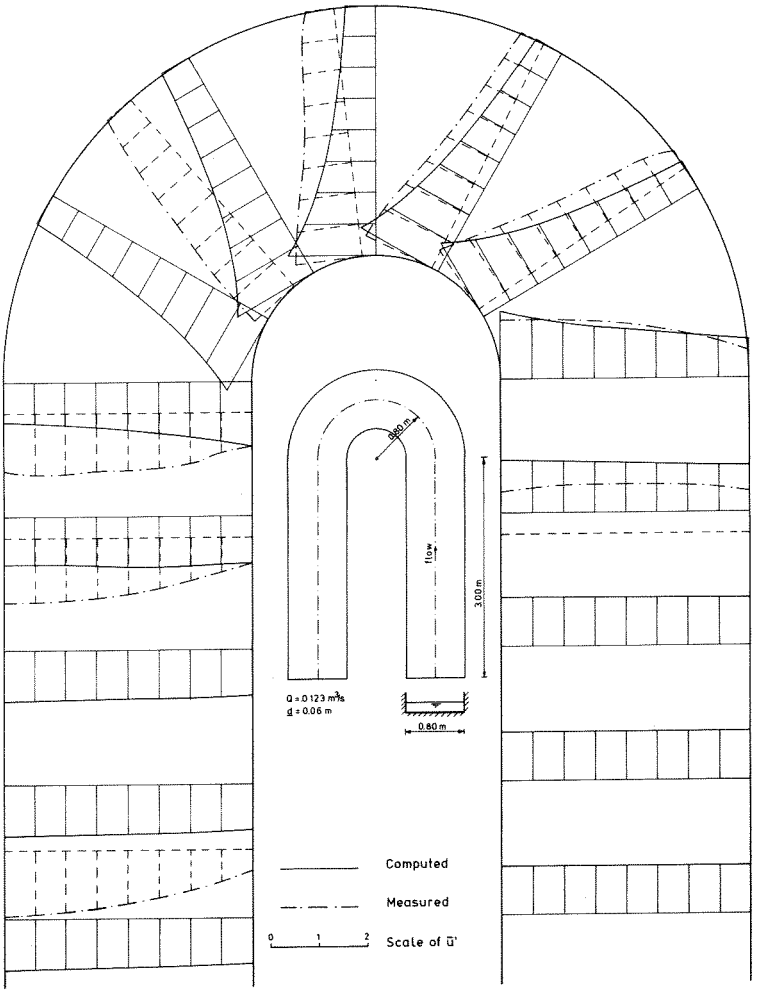

fig. 8a. Velocity-distribution in Rozovs'kii's exp. no. 1

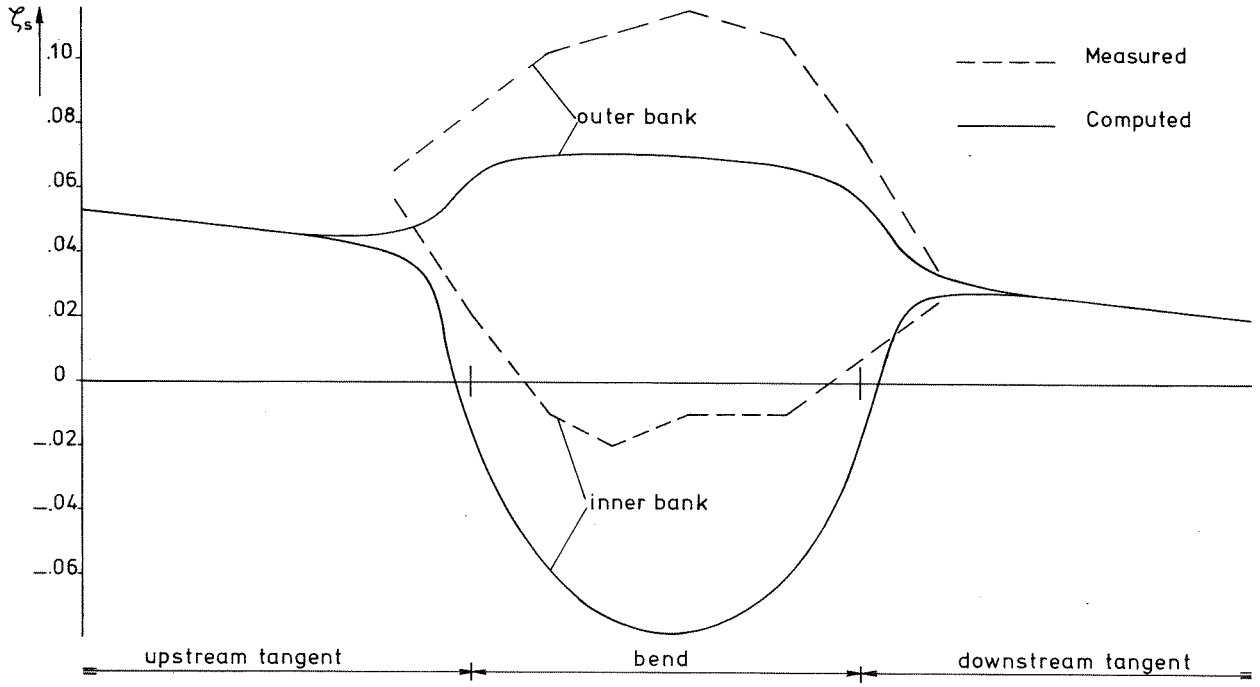

fig. 8b. Water surface elevation

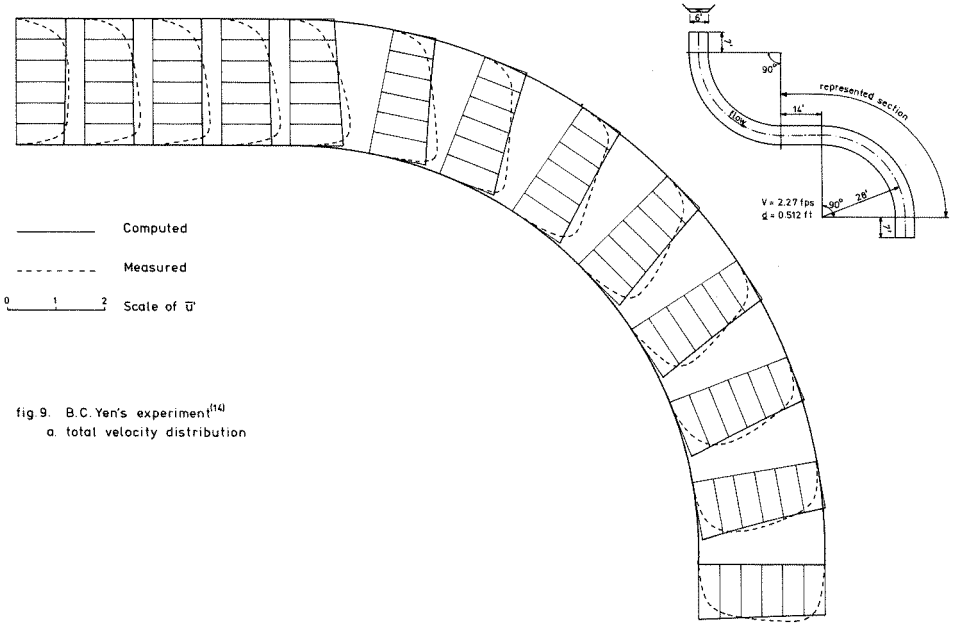

fig. 9. B.C. Yen's experiment[14]
a. total velocity distribution

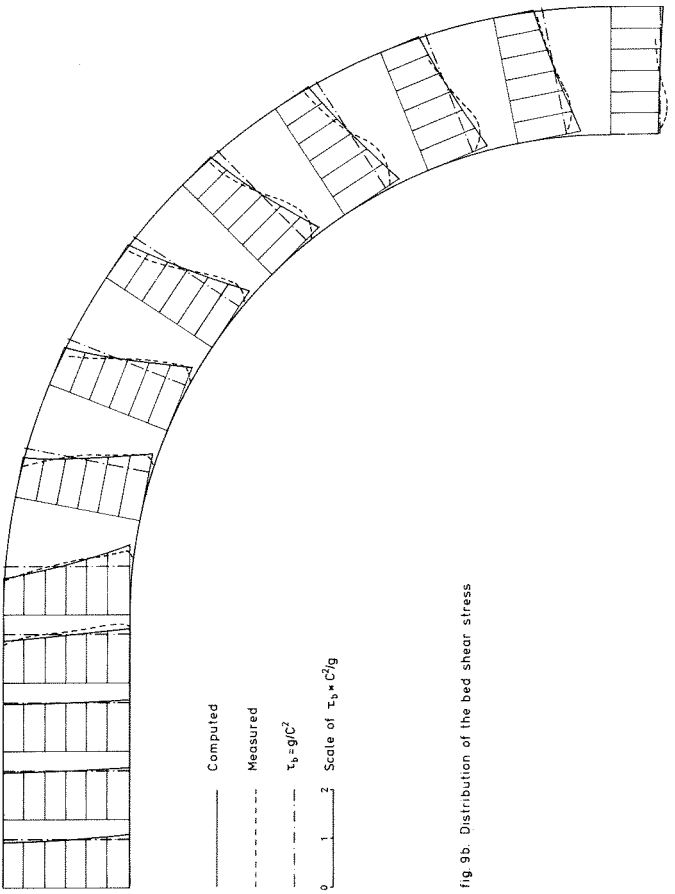

fig 9b. Distribution of the bed shear stress

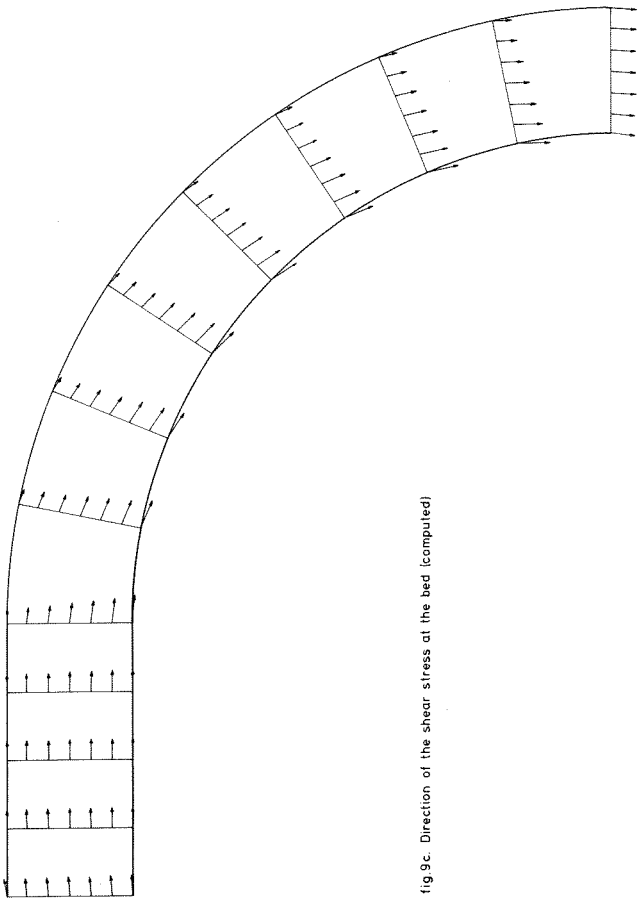

fig.9c. Direction of the shear stress at the bed (computed)

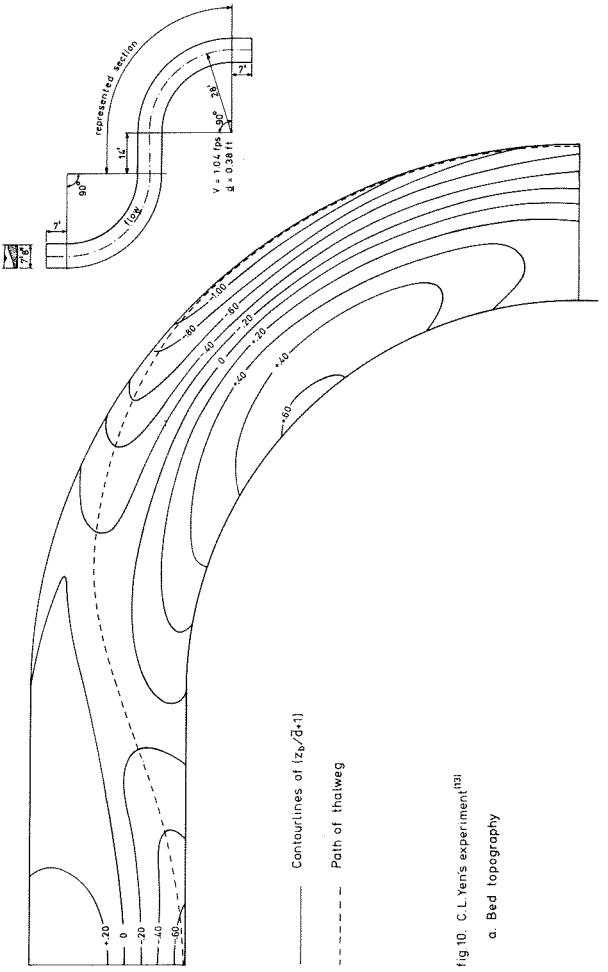

fig 10. C. L. Yen's experiment[131]
a. Bed topography

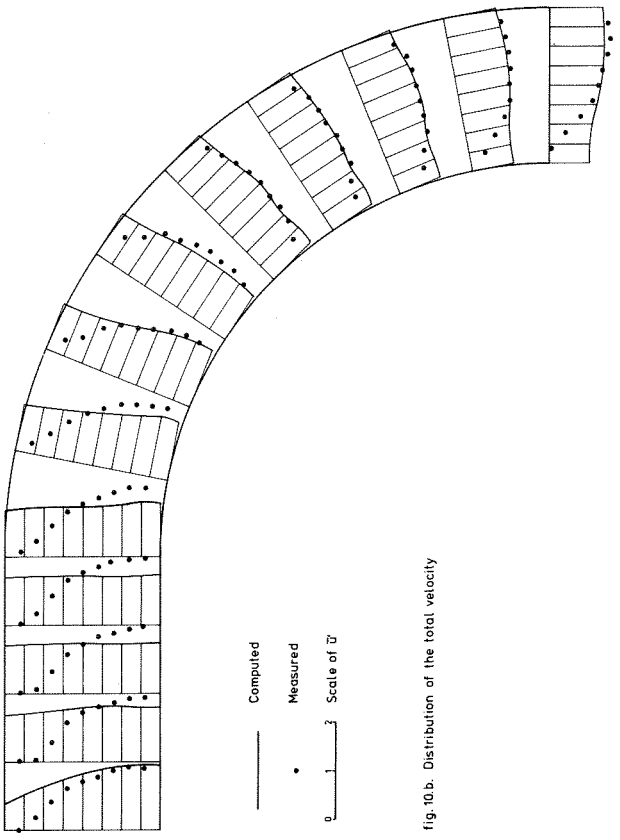

fig. 10.b. Distribution of the total velocity

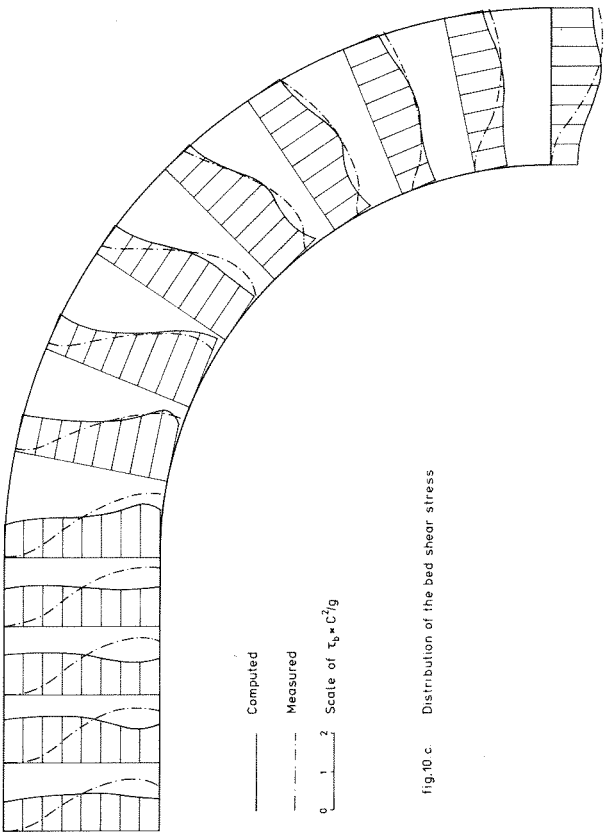

fig.10 c. Distribution of the bed shear stress

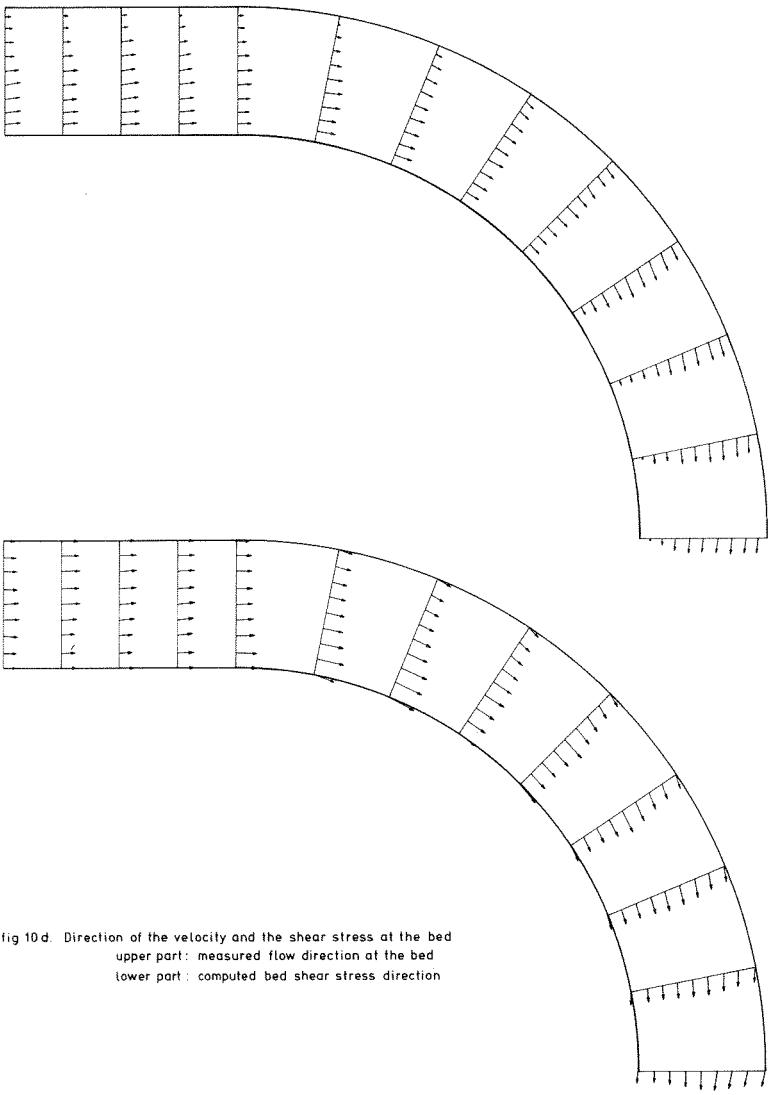

fig 10 d. Direction of the velocity and the shear stress at the bed
upper part : measured flow direction at the bed
lower part : computed bed shear stress direction

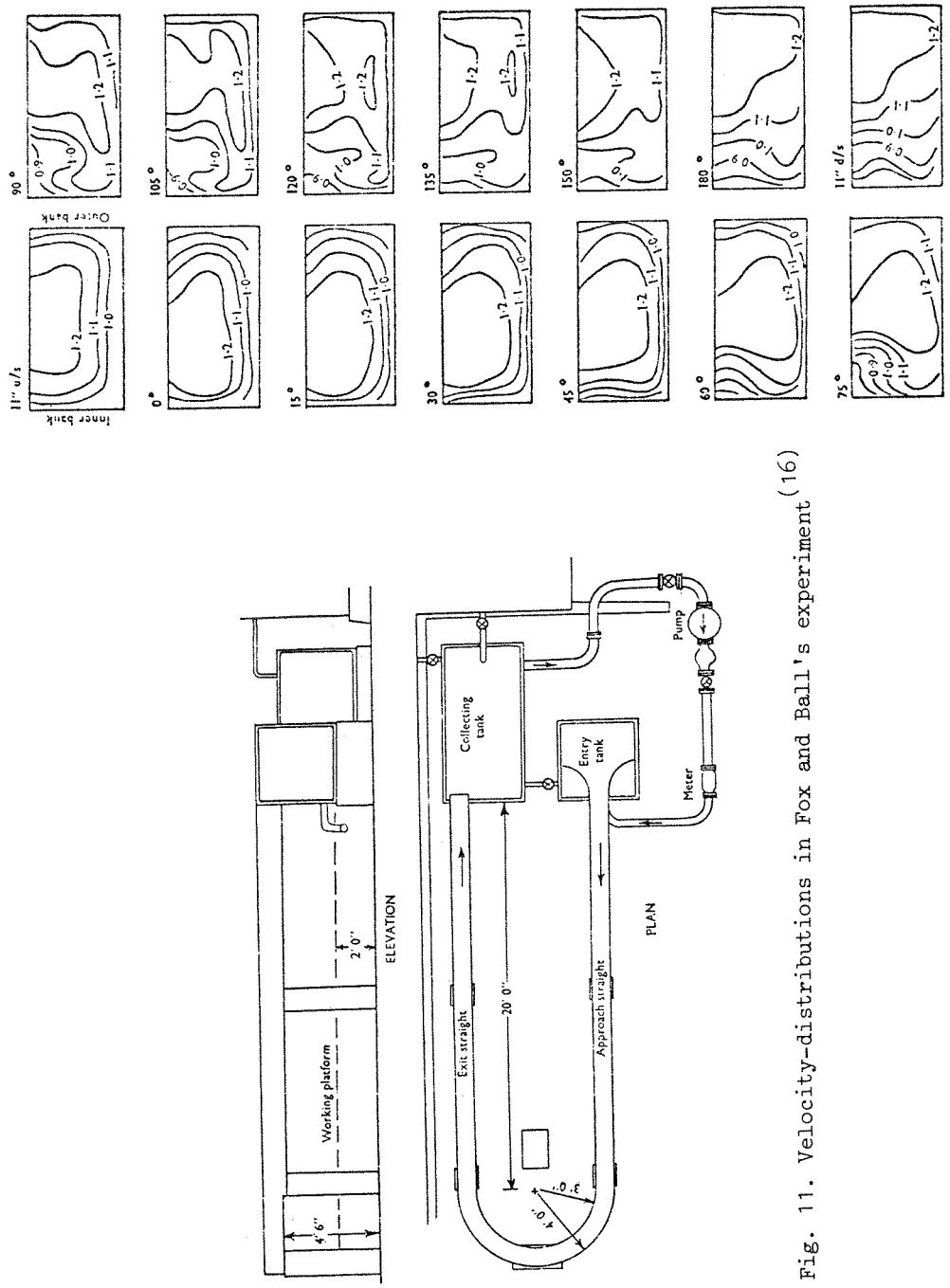

Fig. 11. Velocity-distributions in Fox and Ball's experiment[16]